



## LJMU Research Online

**Abdelrady, H, Hathout, RM, Osman, R, Saleem, IY and Mortada, ND**

**Exploiting gelatin nanocarriers in the pulmonary delivery of methotrexate for lung cancer therapy.**

<http://researchonline.ljmu.ac.uk/id/eprint/10544/>

### Article

**Citation** (please note it is advisable to refer to the publisher's version if you intend to cite from this work)

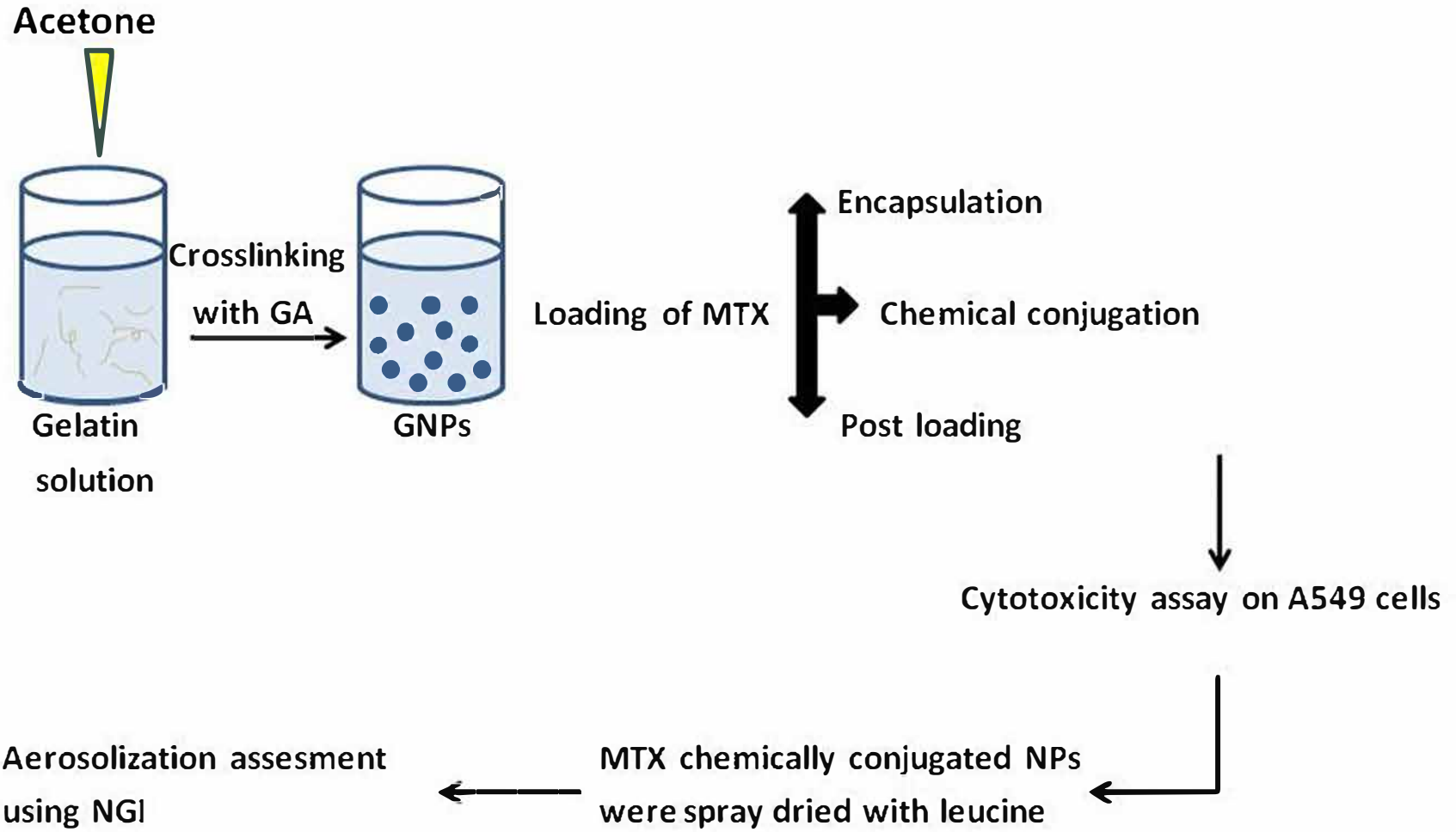
**Abdelrady, H, Hathout, RM, Osman, R, Saleem, IY and Mortada, ND (2019) Exploiting gelatin nanocarriers in the pulmonary delivery of methotrexate for lung cancer therapy. European Journal of Pharmaceutical Sciences, 133. pp. 115-126. ISSN 0928-0987**

LJMU has developed **LJMU Research Online** for users to access the research output of the University more effectively. Copyright © and Moral Rights for the papers on this site are retained by the individual authors and/or other copyright owners. Users may download and/or print one copy of any article(s) in LJMU Research Online to facilitate their private study or for non-commercial research. You may not engage in further distribution of the material or use it for any profit-making activities or any commercial gain.

The version presented here may differ from the published version or from the version of the record. Please see the repository URL above for details on accessing the published version and note that access may require a subscription.

For more information please contact [researchonline@ljmu.ac.uk](mailto:researchonline@ljmu.ac.uk)

<http://researchonline.ljmu.ac.uk/>



# **Exploiting Gelatin Nanocarriers in the Pulmonary Delivery of Methotrexate for Lung Cancer Therapy**

Hend Abdelrady<sup>1,2</sup>, Rania M. Hathout<sup>1</sup>, Rihab Osman<sup>1</sup>, Imran Saleem<sup>2\*</sup>, Nahed D. Mortada<sup>1</sup>

<sup>1</sup> Department of Pharmaceutics and Industrial Pharmacy, Faculty of Pharmacy, Ain Shams University, Cairo, Egypt; <sup>2</sup> School of Pharmacy and Biomolecular Sciences, Liverpool John Moores University, Liverpool, United Kingdom

\*Corresponding Author

Dr Imran Saleem (Liverpool John Moores University, School of Pharmacy & Biomolecular Sciences, Byrom Street, Liverpool L3 3AF, UK; Telephone: +44-151-231-2265; FAX: +44-151-231-1270; E-mail: i.saleem@ljmu.ac.uk).

## Abstract

Gelatin has many merits that encourage its use in the pulmonary delivery of anticancer drugs. It is a biodegradable denatured protein which possesses several functional groups that could be modified. Additionally, it has a balanced hydrophilic and hydrophobic characters, which facilitate the loading of chemotherapeutic agents. Accordingly, the purpose of the current work was to exploit this valuable biomaterial in the efficient pulmonary delivery of methotrexate in case of lung cancer. Gelatin nanoparticles were prepared *via* a desolvation method and the fabrication process was optimized using Box Behnken design of experiment. A comparative study on uptake of gelatin nanoparticles by lung adenocarcinoma cells and macrophages was implemented using flow cytometry. Investigation of the effect of different methotrexate loading techniques: encapsulation, post loading and chemical conjugation on the nanoparticles characteristics and cellular cytotoxicity was performed. Nano-in-microparticles were prepared by *co*-spray drying optimized nanoparticles with leucine. Results showed that Box Behnken design was able to optimize preparation parameters to yield uniform nanoparticles with suitable particle size for cancer cells uptake. The prepared nanoparticles demonstrated a preferential uptake by lung cancer cells. Additionally, methotrexate loaded nanoparticles demonstrated up to four fold significant reduction in methotrexate IC<sub>50</sub>. The spray dried gelatin nano-in microparticles demonstrated good aerosolization properties enabling lung deposition in the respirable airways. Thus, providing a promising platform for lung cancer therapy.

Keywords:

Gelatin, Pulmonary Delivery, Nanoparticles, Methotrexate, Lung Cancer, Spraydrying, Dry Powder Inhalation,

## 1. Introduction:

Lung cancer is by far the leading cause of cancer death among both men and women where it accounts for about 1.59 million deaths globally per year (Novello et al., 2016). Radiotherapy, surgery, chemotherapy or their combinations were the primary therapies for the disease (Mangal et al., 2017). However, conventional intravenous chemotherapy suffer from several drawbacks of such as poor distribution to the lungs accompanied with resistance and metastasis of the cancer cells. Therefore new treatment strategies with improved safety and efficacy such as the pulmonary delivery of nanoparticulate systems are in great demand. It aims at increasing the cytotoxic dose of drugs that could reach tumor cells to improve responses while minimizing systemic toxicity. Additionally, nanoparticulate systems could increase the residence time of chemotherapeutic agent in the lungs accompanied by a prolonged drug release with enhanced cellular internalization (Gill et al., 2011; Taratula et al., 2011; Jyoti et al., 2015).

Gelatin is a natural abundant biomaterial exhibiting unique and promising properties for delivery *via* the pulmonary route. It is obtained by the partial acid and alkaline hydrolysis of animal collagen to yield, respectively, type A with iso-electric point and type B with iso-electric point (Mohanty et al., 2005). Considered as a GRAS (Generally Regarded as Safe) material by the FDA and has been widely used in pharmaceuticals, cosmetics, as well as food products (Mohanty et al., 2005). Gelatin is a polyampholyte having both cationic and anionic groups together with hydrophobic properties in approximate ratio of 1:1:1 that could enhance its ability to load both hydrophilic and hydrophobic drugs (Elzoghby, 2013). Moreover, its functional groups are accessible and can be easily chemically modified, a property which may be useful in developing targeted drug delivery vehicles (Busch, 2003). Gelatin is a denatured protein that could be readily degraded by collagenase enzymes. Additionally, in contrast to collagen, it exhibits low antigenicity (Elzoghby et al., 2012; Elzoghby, 2013; Hathout and Omran, 2016). Overall, its biodegradability, biocompatibility, chemical modification potential and cross-linking possibility make gelatin-based nanoparticles (GNPs) a promising carrier system for drug delivery.

Box Behnken (BBD), is a statistical design of experiment (DoE) which utilizes response surface methodology for the screening and optimization of critical factors in the fabrication of particulate systems. In contrast to traditional one factor at a time experiments (OFAT), DoE offers many advantages as: investigation of several factors at a time, reduction in total number of required experiments and detection of interaction between the investigated process variables (Zhang and Youan, 2010). Additionally, in order to investigate the effect of formulation variables on responses (dependent variables), BBD exclude simultaneous implementation of variables at their maximum or minimum levels, thereby the design points are selected as middle value for one factor and maximum or minimum for the other factors. By avoiding corners in the design space, BBD provides safety in its experiments setting (Marasini et al., 2013). Accordingly, DoE could contribute to enhanced quality attributes of the final product and cost and time reduction of the formulation process (Zhang and Youan, 2010; Marasini et al., 2013; Abdel-Hafez et al., 2014).

Methotrexate (MTX), structure shown in Fig. 1 (Jouyban et al., 2011), is an antimetabolite of folic acid that can inhibit di-hydrofolate reductase enzyme and hence cellular proliferation. MTX influx into the cells is mediated by a reduced folate carrier and /or a proton coupled folate

transporter (Inoue and Yuasa, 2014). It has been used clinically for treatment of many neoplastic disorders and autoimmune diseases such as psoriasis and rheumatoid arthritis (Genestier et al., 2000; Padmanabhan et al., 2009). However, the low tumor accumulation resulting from conventional MTX therapy leads to inefficient treatment, high risk for cancer resistance with a constant need for elevated doses. This is usually opposed by its severe side effects such as myelosuppression, lung distress, nephrotoxicity and ulcerative colitis. Therefore, many passively and actively targeted nanoparticulate carriers *viz* gold, carbon and PLGA nanoparticles (NPs) were proposed to overcome these limitations (Seo et al., 2009; Luo et al., 2014; Afshari et al., 2014; Ajmal et al., 2015).

Despite the great advantages presented by nanoparticulate systems for passive targeted cancer therapy, yet, their mass median aerodynamic diameter (MMAD) is not suitable for pulmonary delivery and they are mostly subjected to exhalation (Yang et al., 2008). Lung deposition is a particle size dependent process where Nano in Microparticles (NIM) with MMAD between 1-5  $\mu\text{m}$  could achieve deposition in the respirable airways (Kunda et al., 2015a; Kunda et al., 2015b). Therefore loading of NPs into a proper pulmonary delivery device should be implemented to enhance its lung deposition efficiency. Dry powder inhaler (DPI) presents many advantages such as; ease of drug administration, independence of actuation-inspiration coordination and enhanced formulation stability. Hence, NPs were incorporated into microparticles using soluble carrier *e.g.* lactose, leucine and trehalose (Bosquillon et al., 2001; Alfagih et al., 2015). NIMs could be prepared using spray drying, freeze drying, spray-freeze drying and super critical fluid technologies (Kunda et al., 2015c; Al-fagih et al., 2011).

In the current work, safe, biodegradable and low-antigenic nanoparticulate gelatin carriers, were designed, characterized and evaluated for their ability to deliver methotrexate. Optimization of the fabrication process was implemented to enhance NPs uptake to the lungs and subsequently cytotoxic effect. Effect of different loading techniques was investigated on drug loading and particles characteristics. Loading of NPs into suitable pulmonary delivery system were implemented to target the lung cancerous sites eliciting a significant cytotoxic response.

## 2. Materials and methods:

### 2.1. Materials

Gelatin type A from porcine skin (Bloom 300), glutaraldehyde solution, glycine, leucine, methotrexate, Phorbol 12-myristate 13-acetate (PMA), *N*-Ethyl-*N'*-(3-dimethylaminopropyl) carbodiimide hydrochloride (EDC), (2-Aminoethyl)tri-methylammoniumchloride hydrochloride, trypsin from bovine pancreas, Roswell Park Memorial Institute medium (RPMI), Dulbecco's Modified Eagle's medium (DMEM) and fluorescein 5-isothiocyanate (FITC) were all purchased from Sigma Aldrich (St. Louis, MO, USA). Acetone of the analytical grade was obtained from Thermofisher (Massachusetts, US). Uranyl acetate was purchased from Agar Scientific (UK). A549 a human lung adenocarcinoma cell line and THP-1 a human monocytic cell line were purchased from American type culture collection ATCC (Manassas, US).

## 2.2. Methods

### 2.2.1. Preparation of gelatin nanoparticles (GNPs)

GNPs were fabricated according to the previously described double desolvation technique (Coester et al., 2000; Azarmi et al., 2006). Briefly, 1.25 g of gelatin were dissolved in 25 mL of de-ionized water at 40°C, and 25 mL of acetone were added to precipitate the high molecular weight fraction (HMwt) of gelatin. The supernatant was discarded and the precipitate was re-dissolved in water under constant heating at 40°C. The pH of the solution was adjusted to 2.5 with 5M HCl. Following on, gelatin solution was secondarily desolvated by dropwise addition of 75 mL of acetone and cross-linking of the prepared NPs was aided using glutaraldehyde solution (25% v/v) under magnetic stirring. Glycine solution (751mg/100ml) was added and stirred at 500 rpm for 1 hour to block the residual aldehyde groups (CHO) of glutaraldehyde and thereby stopping its action. Finally, acetone was removed utilizing a rotary vacuum evaporator and NPs were purified by three fold centrifugation at 30000 rpm, 40 min and 4°C (Optima XPN ultracentrifuge, Beckman Coulter, USA) and re-dispersed in de-ionized water. The resulting GNPs were stored at 4°C for further applications.

### 2.2.2. Optimizing the prepared gelatin nanoparticles using Box Behnken experimental design

Optimization of GNPs preparation process was implemented using the response surface methodology; specifically BBD in order to yield NPs with suitable uniform particle size (PS). Effect of stirring rate, cross-linker solution volume, cross-linking time were studied where three levels for each factor with triplicate center points were selected to create the model, Table 1. Experiments setting and data analysis were performed using Design Expert® v.7.0 (Design Expert® Software, Stat Ease®, MN). The model was evaluated using one-way analysis of variance (ANOVA), lack of fit and regression analysis.

### 2.2.3. Preparation of FITC labeled GNPs

FITC conjugated NPs were fabricated according to a previously described method (T.H.The and T.E.W.Feltkamp, 1970). Briefly, the pH of NPs dispersion in de-ionized water was adjusted to 9.5 using carbonate buffer, 20 µL from (5mg/mL) FITC solution in DMSO was added to GNPs which were then left under magnetic stirring for 4 h at room temperature. Unbound FITC molecules were removed by threefold centrifugation at 30000 rpm, 4°C for 40 min (Optima XPN ultracentrifuge, Beckman Coulter, USA) followed by re-dispersion in de-ionized water.

### 2.2.4. Methotrexate loading

Loading of methotrexate (MTX) was performed on the optimized formulation. The loading process was implemented using three different methods: encapsulation, post loading on cationized GNPs and chemical conjugation in order to evaluate effect of the loading technique on the physical properties and entrapment efficiency of the prepared gelatin NPs.

#### 2.2.4.1. Methotrexate loading using the encapsulation technique

The steps of GNPs preparation were performed as previously stated in section 2.2.1. with drug addition before the second desolvation step where 10 mg of MTX were added to gelatin solution then the amount of acetone was added dropwise. This was followed by addition of glutaraldehyde solution to crosslink the prepared NPs (Bharti et al., 2014).

#### 2.2.4.2. Methotrexate loading using the post-loading technique

Initially, GNPs were cationized according to a previously reported cationization protocol (Zwiorek et al., 2005; Azarmi et al., 2006; Zwiorek et al., 2008), through activation of the free carboxylic groups of gelatin on particles surface to be chemically conjugated with a polyamine compound. Briefly, the pH of GNPs dispersion was adjusted to 4.5 utilizing 0.1 M NaOH and stirred with a molar excess of cholamine hydrochloride for 30 min. An amount of 30 mg of EDC was added and the dispersion was kept under constant stirring overnight. Purification of the NPs was achieved by centrifugation (30000 rpm, 40 min and 4°C) and the pellet was re-dispersed in de-ionized water with the process repeated three times.

Thereafter, 15 mg of cationized NPs were centrifuged and re-suspended in a vial containing (0.125, 0.25, 0.5, 1 and 2 mg/mL) MTX in phosphate buffer solution (PBS) of pH 8 and was left rotating for 1 h at 100 rpm on a Hula mixer (Life Technologies, Invitrogen, UK). Based on the loading results, selected concentration of MTX was then investigated at the respective time points (2, 3, 4 h). Drug loading in each case was analyzed using HPLC as will be explained later and optimum post loading conditions were adopted for further investigations.

#### 2.2.4.3. Methotrexate loading using the chemical conjugation technique

The method was adopted through activation of MTX carboxylic groups to attack free amino groups on NPs surface. Hence, 30mg of EDC were stirred with 10 mg of MTX in PBS (pH 8) for 30 min. then, 60 mg of GNPs were added and left overnight under magnetic stirring (Shin et al., 2014). Validation of MTX chemical conjugation was carried out using proton NMR spectroscopy using Bruker avance III 600 MHz spectrometer with topspin 3.5 software (Bruker, Massachusetts, USA).

### 2.2.5. Characterization of fabricated nanoparticles

#### 2.2.5.1. Determination of the particles yield

To calculate the yield of the optimized formula of GNPs, the HMwt fraction initially precipitated following the first desolvation step was freeze dried for 2 days and weighed. The resultant dispersion of GNPs was also freeze-dried (Heto FD2.5, Heto-Holten, Denmark) over 2 days at -60 °C, 0.065 mbar and then weighed. The yield was calculated for the optimized formulation according to equation (1):

$$Yield(\%) = \frac{\text{Weight of the freeze dried NPs}}{\text{Weight of the HMwt gelatin fraction}} \times 100 \quad \text{Equation (1)}$$

#### 2.2.5.2. Particle size, PDI and zeta potential

Mean particle size (PS), polydispersity index (PDI) and zeta potential ( $\zeta$ ) measurement were carried out for the prepared NPs using dynamic light scattering (DLS) technique for PS and PDI and laser Doppler velocimetry for  $\zeta$  (Zetasizer, Malvern, UK). All measurements were carried out in triplicates, means and standard deviations (SD) were also calculated. The effect of pH on  $\zeta$  of GNPS and cationized GNPs was determined also by laser Doppler velocimetry. For the measurement, pH of the NPs dispersion was adjusted to values between 2.5 and 10 using 0.25 N HCl or 0.25 N NaOH.

### 2.2.5.3. Determination of drug loading

The drug content in the prepared GNPs was determined indirectly by analyzing the amount of free drug remaining in the supernatant after centrifugation of the loaded NPs according to a previously described high performance liquid chromatography (HPLC) validated method (Oliveira et al., 2015). Briefly, an HPLC instrument equipped with UV-visible detector was set to 303 nm. Hypersil BDS C18 column and a mobile phase consisting of methanol and ammonium acetate buffer (pH 6) with a ratio of (25:75) were selected for the separation technique. At 25°C, an isocratic elution was utilized with a flow rate of 1mL/min. MTX loading was calculated using equation (2):

$$\text{Drug loading} \left( \frac{\mu\text{g}}{\text{mg of NPs}} \right) = \frac{\text{Initial drug amount} - \text{remaining drug amount}}{\text{amount of gelatin}} \quad \text{Equation (2)}$$

### 2.2.5.4. *In-vitro* drug release

MTX loaded NPs dispersion equivalent to 20 mg of NPs were mounted into dialysis bags (MWCO 3500 D) and dialyzed against 50 mL of PBS (pH 7.4) for 72 h. NPs dispersion and dialysis media were kept under continuous magnetic stirring at 37 °C. Samples were withdrawn at fixed time intervals and were replaced with fresh PBS. Investigation of the release in the presence of a proteolytic enzyme was also accomplished. Therefore, the NPs were accompanied by 10 mg of trypsin in the dialysis bag. Samples were analyzed for the amount released of MTX utilizing HPLC as previously described in section 2.2.5.3. For evaluation of the release kinetics, the obtained release data were fitted into the Korsmeyer-Peppas exponential equation (3) in order to determine the mechanism of drug release

$$Q = Kt^n \quad \text{Equation (3)}$$

Where  $Q$  is the percentage of drug released at time  $t$  and  $k$  is a constant incorporating the structural and geometric characteristics of the investigated dosage form. The diffusional exponent  $n$  is an indicator of the mechanism of drug transport from the dosage form. A value of  $n \leq 0.5$  indicates that drug release is controlled by Fickian diffusion, whereas a value of  $0.5 > n > 1$  the release is described as anomalous, implying that a combination of diffusion and erosion contributes to the control of drug release (Costa and Lobo, 2001).

### 2.2.5.5. Flow cytometry experiment

A comparative uptake of FITC-labeled GNPs into lung adenocarcinoma (A549) cells and macrophages (THP-1) were evaluated using flow activated cell sorting (FACS). THP-1 human monocyte cells were differentiated into macrophages using PMA as follow: the cells were seeded into 6 well plates at a density of  $1 \times 10^6$  cells per well, and were then incubated in RPMI medium containing 50 ng/mL PMA for 48 h. Unattached cells were removed and washed with PBS three times (Takashiba et al., 1999; Park et al., 2007). A549 human lung adenocarcinomic cells were plated at density of  $1 \times 10^6$  cells per well into a 6 well culture plate and were maintained in DMEM medium.

Macrophages and lung adenocarcinomic cells were treated each with 4 mg of FITC labeled GNPs suspended in 3mL of RPMI and DMEM media, respectively. After 4 h of incubation at 37°C, the treated cells were washed three times with phosphate buffer saline (pH 7.4), trypsinized and re-suspended in fresh media. Flow cytometric analysis was performed using a flow cytometer (BD Accuri™ C6 flow cytometer, BD Biosciences, US). The data were analyzed using BD Accuri C6 software by gating on live cell population with a minimum of 10000 events were recorded. Median FLA-1 was chosen for comparative fluorescence changes. Median FLA-1 was compared in macrophages and A549 cells before and after treatment with FITC- labeled GNPs.

#### 2.2.5. 6. *In-vitro* cytotoxicity assay

Cell viability was investigated using MTT assay. A549 cells were seeded into 96 well plates at a density of  $1 \times 10^4$  cell per well in DMEM media supplemented with 10% Fetal serum protein, 100 IU/mL penicillin and 100 mg/mL streptomycin. They were incubated at 37°C in an atmosphere of 5% CO<sub>2</sub> for 24 h. Cells were then treated with serial concentrations of MTX loaded GNPs, blank GNPs, cationized GNPs and free MTX solution in PBS (pH 7.4). Additionally, 10% DMSO and fresh medium were utilized as positive and negative controls, respectively. Following 24 h of incubation, the cells were washed with phosphate buffer saline and 100 µL of fresh medium and 20 µL of MTT solution (5mg/mL MTT) were added. After 4 h of incubation, the formed formazan crystals were dissolved with 100 µL DMSO. Absorbance in each well was measured by Clariostar plate reader (BMG Labtech, Germany) at 570 nm (Osman et al., 2013; Afshari et al., 2014). % Cell viability was calculated according to the following equation:

$$\% \text{ cell viability after 24 h incubation} = \frac{\text{absorbance of treated cell with GNPs} \times 100}{\text{absorbance of untreated cell (control)}} \text{ Equation (4)}$$

#### 2.2.6. Preparation of spray dried nano-in microparticles (NIM)

Freshly prepared optimized MTX loaded NPs were spray dried using leucine as carrier at a ratio of 1:1.5, respectively. Büchi B-290 mini spray-dryer (Büchi Labortechnik, Flawil, Switzerland) was used at a pump capacity of 20% and an atomizing air flow of 414 L/h. The dry particles were separated from the air stream using a high-performance cyclone (Büchi Labortechnik, Flawil, Switzerland) where they were collected and stored in a desiccator until further use. Preparation of spray dried NIM was implemented at variable conditions of temperature (75-100-125°C), aspiration rate (50-75-100%) and feed concentration (4-8-12mg/mL) after proper dilution with water in order to optimize the yield and residual moisture in the spray dried NIM using BBD. Supplementary material Table 2 shows the formulae prepared for this optimization study.

## 2.2.7. Characterization of spray dried NIM

### 2.2.7.1. Spray dried powder yield

The percentage yield of dry powder was calculated according to equation (5):

$$\text{Yield (\%)} = \frac{\text{Weight of powder collected after spray drying}}{\text{Weight of total dry mass used for the preparation}} \times 100 \quad \text{equation (5)}$$

### 2.2.7.2. Moisture content determination

The moisture content of the spray dried NIM was evaluated using thermo-gravimetric analysis (TGA Q50, UK equipped with TA universal 2000 software). Briefly, 10 mg of the powder were heated between 25 and 350°C at a rate of 15 °C per min. Data analysis for residual moisture were investigated between 25 to 120°C.

### 2.2.7.3. Particles morphology

Spray dried powders were visualized using scanning electron microscopy (SEM) (FEI Quanta™ 200 ESEM, Holland). Samples were mounted on aluminium stubs (pin stubs, 13 mm) layered with a sticky conductive carbon tab and coated with palladium (10–15 nm) using a sputter coater (EmiTech K 550X Gold Sputter Coater, 25 mA).

### 2.2.7.4. Nanoparticles recovery

To ensure the recovery of NPs from spray dried powder with suitable PS for cellular uptake, an aliquot of 5 mg of spray dried powder was dispersed into 2 mL of deionized water. PS, PDI and  $\zeta$  were measured for the released NPs. Moreover, the particles were stained with uranyl acetate and visualized using transmission electron microscopy (TEM), electron micrographs were recorded using a MegaView3 CCD camera and AnalySIS software (EMSIS GmbH, Germany) in a FEI Tecnai G2 spirit BioTWIN electron microscope.

### 2.2.7.5. *In-vitro* aerosolization studies

Aerosolization performance of spray dried gelatin NIM was assessed using the next generation impactor (NGI). An accurately weighed amount (20 mg) of spray dried gelatin NIM were filled into each hydroxypropyl methylcellulose capsule (size 3), 10 capsules were used for each run and the experiment was performed in triplicate. Capsules were punctuated with Cyclohaler and aerosolized into the NGI (Copley scientific pump, Nottingham, UK) at a flow rate of 60 L/min for 4 seconds. NGI plates were coated with 1% glycerol in acetone to prevent bouncing of fine powders between plates (Tawfeek et al., 2013). The plates were weighted before and after aerosolization of the powders (Sham et al., 2004). Mass median aerodynamic diameter (MMAD) was calculated using log probability analysis. Respirable fraction is the fraction of emitted dose deposited in the NGI with  $d_{ae} < 4.46 \mu\text{m}$ . Emitted and respirable fraction were calculated according to the following equations:

$$\text{Emitted fraction (EF\%)} = \frac{M_{full} - M_{empty}}{M_{powder}} \times 100 \quad \text{Equation (6)}$$

Where  $M_{full}$  and  $M_{empty}$  are the masses of the capsules before and after aerosolization, respectively.  $M_{powder}$  is the mass of the powder.

$$\text{Respirable fraction (RF\%)} = \frac{FPD}{ED} \times 100 \quad \text{Equation (7)}$$

Where fine particle dose (FPD) is the total weights of powder deposited from plate number 2 to plate number 7. Emitted dose (ED) could be calculated as the difference between the mass of the capsule before and after aerosolization  $M_{full} - M_{empty}$ .

### 2.2.8. Statistical analysis

All data are reported as mean of 3 determinations  $\pm$  standard deviation (SD). Experiments setting and data analysis for GNPs and spray dried NIM optimization were performed using Design Expert<sup>®</sup> v.7.0 (Design Expert<sup>®</sup> Software, Stat Ease<sup>®</sup>, MN). Other data obtained were analysed statistically by one-way ANOVA and two-way ANOVA was utilized for statistical analysis of NPs uptake data. Statistical significant difference was noted when  $p < 0.05$ .

## 3. Results and discussion

### 3.1. Optimization of the prepared GNPs

In pulmonary delivery, cellular uptake of passively targeted nanoparticulate carriers is a size dependent process where NPs with mean PS between 100–200 nm could be preferably endocytosed by cancerous cells (Nagayasu et al., 1999; Kulkarni and Feng, 2013; Abozeid et al., 2016). Accordingly, optimization of preparation conditions was implemented using BBD to yield NPs possessing PS suitable for lung cancerous cells endocytosis.

All the prepared formulations demonstrated a mean PS ranging from  $180.31 \pm 10.10$  to  $469.56 \pm 7.37$  nm as shown in Table 2. The obtained responses were fitted to a proper reduced quadratic model after elimination of the insignificant terms ( $p > 0.05$ ) from the model equation. The equation describing the resultant quadratic model was found to be:

$$Y = 268.71 - 36.34 * A - 36.9 * B - 30.44 * C + 60.83 * A * B + 58.24 * B^2 - 23.35 * C^2 \quad \text{Equation (8)}$$

Where Y is the PS, A is the cross-linking solution volume, B is the cross-linking reaction time, and C is the stirring speed.

The response surface reduced quadratic model was significant with respect to these model terms; A, B, C, AB,  $B^2$  and  $C^2$ . Model reliability was verified utilizing ANOVA, lack of fit test and regression analysis. Regarding the ANOVA test, the obtained p-value was less than 0.05, actually scoring a value of 0.0001, see supplementary material Table 1. Moreover, the lack of fit test, demonstrating adequacy of the model to represent the variation of the generated responses,

depicted a p-value of 0.0790 indicating favorable “insignificant results” (Safwat et al., 2017; Naguib et al., 2017) supplementary material Table 1. In regression analysis as shown in supplementary material Table 1, the  $R^2$  and the adjusted  $R^2$  values indicate the variation of the results around the mean introduced by the model and their fitting to the reduced corrected model, respectively. Predicted  $R^2$  is a measure of how efficient the model predicts a new observation. The adjusted  $R^2$  and predicted  $R^2$  were within 0.2 of each other to be in a reasonable agreement. Finally, adequate precision is a measure of the experimental signal to noise ratio. The adequate precision scored 24.848, a value higher than the critical value of 4, indicating high signal to noise ratio and sufficiency of the model to navigate the experimental space (Zhang and Youan, 2010; Marasini et al., 2013; Abdel-Hafez et al., 2014). Consequently, the model could be utilized for GNPs size optimization and prediction.

Fig. 2 represents the contour and 3D plots of the model. It is obvious that increasing the cross-linking solution volume and stirring speed were associated with a significant reduction in PS of the resulting NPs. This can be ascribed to glutaraldehyde that is essential for gelatin assembly into nanospheres, stability and hardening (Azarmi et al., 2006; Elzoghby, 2013). Moreover, the shearing force from higher stirring speeds helps in particles rounding and spheronization (Dinarvand et al., 2004; Jahanshahi et al., 2008). Additionally, a moderate cross-linking time was selected, this can be justified by the fact that the increase in reaction time could enhance probability of interparticulate cross-linking (Wong et al., 2011). Hence, the optimized preparation conditions were: stirring speed of 1600rpm, cross linking time of 12 h and cross linking solution volume of 231  $\mu$ L, (Table 2) which resulted in a formulation with mean PS of  $180.31 \pm 10.10$ nm, PDI of  $0.05 \pm 0.03$  and  $\zeta$  of  $18.50 \pm 1.81$  mV, which was selected for further investigations. Furthermore, a desirable yield of  $84.18 \pm 0.26$  % from the HMwt gelatin fraction was obtained.

### 3.2. Methotrexate loading

The effect of loading technique on the characteristics of MTX loaded NPs in terms of PS, PDI,  $\zeta$  and MTX loading, is displayed in Table 3. It can be seen that a negligible loading was observed in the NPs prepared with encapsulation technique compared with other techniques. This may be explained due to MTX moderate solubility in acetone accompanied with long stirring time, which could enhance its leakage from the NPs during fabrication.

Concerning post loaded NPs, due to the polyampholytic nature of gelatin and MTX, the pH of their dispersion medium controls the charge they carry, consequently, the electrostatic attraction between NPs and the drug then the loading efficiency. As shown in Fig. 3A, cationization of gelatin was carried out in order to preserve its positive net charge during post loading at pH 8, as previously addressed by (Zwiorek et al., 2005). Whereas MTX will acquire a negative charge at this pH and could be electrostatically attracted to the NPs. Figure 3B demonstrates the effect of MTX concentration on the amount adsorbed per mg of NPs. Expectedly, a significant increase in loading was observed with higher concentrations at 1 hour as a higher amount of MTX was available for adsorption. Furthermore, Fig. 3C shows a maximum loading of MTX at 1 hour with no significant change in the loading with longer time periods ( $p > 0.05$ ). This may be attributed to

saturation of the NPs to adsorption (Kunda et al., 2015). For MTX post loaded NPs preparation, cationized GNPs was stirred with 2mg/ML of MTX for 1h. Effective MTX adsorption to cationized NPs could be indicated by the reduction in  $\zeta$  of the cationized NPs from  $18.08 \pm 1.02$  at pH 8 to  $14.03 \pm 0.05$  mV by the negatively charged adsorbed MTX ( $p < 0.05$ ) (Shutava et al., 2009).

In another approach, MTX was chemically conjugated to NPs through amide bond formation that was assisted by EDC activation of MTX carboxylic group. In Fig. 4, the NMR charts depicts that the peaks at 6.8, 7.75 and 8.58 ppm of MTX were also present in the chemically conjugated gelatin and normally absent in gelatin (Fu et al., 2017) indicating that MTX was successfully conjugated. Moreover, the minimal PS reduction of the chemically conjugated NPs compared with blank gelatin NPs ( $p < 0.05$ ) could be attributed to the longer stirring time that NPs were subjected to it, which may enhance particles rounding and spheronization. Based on the loading results NPs loaded by encapsulation were excluded from further studies.

### 3.3. *In-vitro* drug release results

In fig. 5, drug release results from post loaded NPs reveal an initial burst release of  $43.25 \pm 1.18$  % of MTX during the first 8 h that was followed by a sustained release with a slower rate for 24 h, then no release was noticed until 72 h. On the other hand, a higher initial release of MTX ( $58.90 \pm 4.1$  %) and almost a complete drug release was observed after 36 h in the presence of trypsin. On the other hand, no release of MTX from the chemically conjugated NPs was observed in the absence of trypsin. In contrary upon its addition, where only  $35.71 \pm 3.66$  % was released to the recipient compartment during 72 h. Enhancement of drug release from the prepared NPs in the presence of trypsin could be attributed to the proteolytic action of trypsin that degraded GNPs into small fragments causing MTX release (Abozeid et al., 2016). Degradation of GNPs occur either after endocytosis or by extracellular proteases. The Gly-X-Pro sequence (where X represents lysine, arginine, methionine and valine) that is responsible for the triple helical structure of gelatin, is initially attacked by collagenase enzyme which is followed by further degradation that is implemented by other enzymes like gelatinase and other non specific proteinases (Abozeid et al., 2016). However, incomplete drug recovery from chemically conjugated NPs could be explained by, upon enzymatic degradation of NPs, only free MTX molecules and/or MTX- peptide fragments of molecular weight lower than 3500 daltons (cut off value of the dialysis membrane) could be released from the dialysis bag. Where only free MTX molecules could be analyzed in the release medium (Leo et al., 1999).

The release kinetics was evaluated by fitting the obtained data (during the first 24 h) into Korsmeyer-Peppas equation. Based on the results, MTX release from the post loaded NPs recorded an (n) exponent of 0.37 and  $R^2$  of 0.93, which suggest that a Fickian diffusion process is predominant. This could be attributed to the strong electrostatic attraction between the cationic GNPs and negatively charged MTX molecules which could control the drug diffusion to the surrounding medium (Shutava et al., 2009). MTX release from post loaded ( $n=0.69$ ,  $R^2=0.95$ ) and chemically conjugated NPs ( $n=0.57$ ,  $R^2=0.96$ ) in the presence of trypsin demonstrated an anomalous transport. This could be attributed to the erosion of gelatin matrix by the enzymatic degradation (Gao et al., 2013). It is worth mentioning that despite of the release mechanism of

MTX from the GNPs, the NPs were designed to be uptaken by the cancerous cells as demonstrated in the following section. The release profiles confirmed the ability of the NPs to hold the drug sufficiently until cellular uptake.

### 3.4. Gelatin nanoparticles uptake

Lung macrophages are one of the major host defense mechanisms and a serious determinant for the fate of NPs delivery to the lungs. Therefore, to ensure optimum activity and cytotoxic efficiency of the prepared NPs, a comparative uptake of GNPs was evaluated between the macrophages and the lung adenocarcinoma cells by flow cytometry. Figure 6 and Table 4 illustrate the fluorescence changes reflected by median FLA-1 between cells treated with FITC- labeled NPs and control untreated cells, where median FLA-1 of A549 treated cells was significantly elevated compared to the macrophages counterpart ( $p < 0.05$ ). This may be attributed to, the fact that phagocytosis is a PS dependent process where particles less than 260 nm tend to escape from phagocytic clearance (Yang et al., 2008) whereas FITC- labeled NPs had a mean PS of  $188 \pm 6.20$  nm as in Table 3. Additionally, cancerous cells shows a favorable uptake to NPs between 100–200 nm (Nagayasu et al., 1999; Kulkarni and Feng, 2013). This was correlated with the results obtained by Azarmi, (Azarmi et al., 2006), where three groups of GNPs with sizes of 190, 283 and 330 nm were investigated for their uptake into osteosarcoma cells. GNPs with size of 190 nm showed the highest uptake into osteosarcoma cell line. In addition, GNPs prepared with PS of 260 or higher demonstrated significant uptake into macrophage cells (Coester et al., 2000; Coester et al., 2006).

### 3.5. Cytotoxicity assay

MTT assay was utilized to investigate toxicity profiles of MTX loaded NPs on the adenocarcinomic A549 cell lines. Both blank gelatin and cationized NPs were well tolerated by the cells up to concentration of 2 mg/mL showing cell viabilities of  $85 \pm 2.61\%$  and  $80 \pm 1.5\%$ , respectively as previously reported by (Metwally et al., 2016). Furthermore, Fig. 7 demonstrates that post loading and chemical conjugation of MTX to gelatin NPs could effectively enhance its cytotoxic activity and reduce its  $IC_{50}$  by two and four folds, respectively. The enhanced activity of the post loaded NPs compared to free MTX could be explained by the higher amounts of MTX that could be delivered by NPs to the cells. Consequently, a greater cytotoxic effect and lower  $IC_{50}$  values were observed (Afshari et al., 2014). Chemically conjugated NPs showed lower  $IC_{50}$  compared to post loaded NPs, this could be attributed to smaller PS of chemically conjugated NPs which may promote their uptake by the A549 cells (Nagayasu et al., 1999; Kulkarni and Feng, 2013). In addition, MTX is an analogue to folic acid which may promote NPs targeting and receptor mediated endocytosis to over expressed folate receptors in cancerous cells (Luo et al., 2014). Therefore, MTX chemically conjugated NPs were selected for spray drying and DPI preparation.

### 3.6. Preparation of spray dried NIM

As previously discussed, despite the many advantages addressed by the NPs when utilized for lung cancer treatment, however large fraction of NPs could be exhaled easily due to its MMAD is not suitable for the pulmonary delivery. Therefore, spray drying of the optimized formula with leucine was adopted to enhance its delivery to lower respiratory tract regions *via* DPI.

Based on the applied process variables, the yield and moisture content varied from  $19.0 \pm 5.90$  to  $84.50 \pm 6.80\%$  and from  $0.56 \pm 0.05$  to  $1.32 \pm 0.50\%$ , respectively, see Table 2 supplementary material. The results of data analysis according to the BBD are shown in Table 3 supplementary material. The design analysis revealed that the yield increased with increasing the 3 investigated factors while the moisture content decreased with increasing temperature and feed concentration. The 3D contour plots of the effects of the various variables are presented in Fig. 1 supplementary material. Accordingly, the following conditions were selected: inlet temperature of  $125\text{ }^{\circ}\text{C}$ , aspirator capacity of 100 % and a feed concentration of 8 mg/mL. Hence, a desirable yield of  $84.50 \pm 6.80$  (%) was obtained. Moreover, the low moisture content  $0.98 \pm 0.28$  (%) reported from the TGA thermogram presents a good drying efficiency therefore the dry powder formulations are likely to show good storage stability and dispersibility.

### 3.7. Characterization of spray dried NIM

#### 3.7.1. Particles morphology

SEM of spray dried GNPs, Fig. 8 A&B show irregular particles possessing a notch in its center and a rough outer surface. This doughnut shape could be attributed to the accelerated rate of evaporation due to the high inlet temperature that led to trapping of excessive amounts of vapour inside the particle (Yang et al., 2015).

#### 3.7.2. Recovery results of the nanoparticles

The released NPs from spray dried powder, had a mean PS of  $160 \pm 9.78$  nm, PDI of  $0.183 \pm 0.004$  and  $\zeta$  of  $-23 \pm 0.15$  mV that were insignificantly different from those obtained for the MTX chemically conjugated NPs before spray drying at ( $p > 0.05$ ). Furthermore, as demonstrated from the TEM in Fig. 8 C&D, there was no visual difference in shape of the NPs before and after re-dispersion from spray dried powder. Accordingly, spray drying conditions were able to preserve NPs characteristics and consequently their cellular uptake.

#### 3.7.3. *In-vitro* aerosolization studies

Powder deposition results presented a powder recovery from the cyclohaler of  $96.08 \pm 0.38$  (%), MMAD of  $2.59 \pm 0.31$   $\mu\text{m}$  and a respirable fraction of  $49.53 \pm 2.10$  (%), suggesting a lung deposition in the respirable airways. This has been ascribed to the hydrophobic alkyl chain of leucine as a carrier which could reduce the microparticles cohesive interparticulate interactions and surface energy (Tawfeek et al., 2011). In addition, the particles rough surface that resulted in particles with minimal sites for interparticulate crosslinking, hence it demonstrated enhanced

dispersibility during aerosolization (Tawfeek et al., 2011). Moreover, the lower residual moisture in spray dried particles which could be favorable for particles flowability (Tawfeek et al., 2011). Similar reports have also demonstrated the enhanced aerosol performance with leucine containing formulations (Najafabadi et al., 2004; Feng et al., 2011; Sou et al., 2013).

#### 4. Conclusion

Optimization of GNPs preparation parameters could be implemented with Box Behnken design, to yield NPs with suitable particle size for lung cancer cells uptake and cytotoxic efficiency. Moreover, an enhanced uptake of the gelatin NPs by the lung adenocarcinoma cells compared to macrophages was confirmed which could facilitate the chemotherapeutic agents' delivery to the cancerous tissues. Consequently, investigation of different techniques in loading of MTX and cytotoxicity assays of the resultant formulations were carried out. The chemical conjugation of MTX to gelatin NPs could successfully augment the cytotoxic activity of MTX compared to the free drug and the NPs prepared using other techniques. Finally, spray drying of MTX chemically conjugated NPs showed good aerosolization properties and lung deposition in the broncho- alveolar airways.

#### Acknowledgement

Hend Abdelrady would like to thank the Egyptian Ministry of Higher Education, for funding her research studies at Liverpool John Moores University.

## References

Abdel-Hafez, S.M., Hathout, R.M., Sammour, O.A., 2014. Towards better modeling of chitosan nanoparticles production: Screening different factors and comparing two experimental designs. *Int. J. Biol. Macromol.* 64, 334-340.

Abozeid, S.M., Hathout, R.M., Abou-Aisha, K., 2016. Silencing of the metastasis-linked gene, AEG-1, using siRNA-loaded choline surface-modified gelatin nanoparticles in the breast carcinoma cell line MCF-7. *Colloids Surf. B. Biointerfaces.* 145, 607-616.

Afshari, M., Derakhshandeh, K., Hosseinzadeh, L., 2014. Characterisation, cytotoxicity and apoptosis studies of methotrexate-loaded PLGA and PLGA-PEG nanoparticles. *J. Microencapsul.* 31, 239-245.

Ajmal, M., Yunus, U., Matin, A., Haq, N.U., 2015. Synthesis, characterization and in vitro evaluation of methotrexate conjugated fluorescent carbon nanoparticles as drug delivery system for human lung cancer targeting. *J. Photochem. Photobiol. B.* 153, 111-120.

Al-fagih, I.M., Alanazi, F.K., Hutcheon, G.A., Saleem, I.Y., 2011. Recent Advances Using Supercritical Fluid Techniques for Pulmonary Administration of Macromolecules via Dry Powder Formulations. *Drug Del. Lett.* 1, 128-134.

Alfagih, I., Kunda, N., Alanazi, F., Dennison, S.R., Somavarapu, S., Hutcheon, G.A., Saleem, I.Y., 2015. Pulmonary Delivery of Proteins Using Nanocomposite Microcarriers. *J. Pharm. Sci.* 104, 4386-4398.

Azarmi, S., Huang, Y., Chen, H., McQuarrie, S., Abrams, D., Roa, W., Finlay, W.H., Miller, G.G., Lobenberg, R., 2006. Optimization of a two-step desolvation method for preparing gelatin nanoparticles and cell uptake studies in 143B osteosarcoma cancer cells. *J. Pharm. Pharm. Sci.* 9, 124-132.

Bharti, N., Harikumar, S.L., Shishu, Buddiraja, A., 2014. Formulation and Evaluation of gelatin nanoparticles for pulmonary drug delivery. *World J. Pharm. Pharm. Sci.* 3, 733-744.

Bosquillon, C., Lombry, C., Preat, V., Vanbever, R., 2001. Influence of formulation excipients and physical characteristics of inhalation dry powders on their aerosolization performance. *J. Control. Release.* 70, 329-339.

Busch, S., Schwarz, U., Kniep, R., 2003. Chemical and Structural Investigations of Biomimetically Grown Fluorapatite–Gelatin Composite Aggregates. *Adv. Funct. Mater.* 13, 189-198.

Coester, C., Nayyar, P., Samuel, J., 2006. In vitro uptake of gelatin nanoparticles by murine dendritic cells and their intracellular localisation. *Eur. J. Pharm. Biopharm.* 62, 306-314.

Coester, C.J., Langer, K., van Briesen. H., Kreuter, J., 2000. Gelatin nanoparticles by two step desolvation--a new preparation method, surface modifications and cell uptake. *J. Microencapsul.* 17, 187-193.

Costa, P., Lobo, J., 2001. Modeling and comparison of dissolution profiles. *Eur. J. Pharm. Sci.* 13, 123-133.

Dinarvand, R., Mahmoodi, S., Farboud, E., 2004. Effect of process variables on particle size of gelatin microspheres containing lactic acid. *Pharm. Dev. Technol.* 9, 291-299.

Elzoghby, A.O., 2013. Gelatin-based nanoparticles as drug and gene delivery systems: reviewing three decades of research. *J. Control. Release.* 172, 1075-1091.

Elzoghby, A.O., Samy, W.M., Elgindy, N.A., 2012. Protein-based nanocarriers as promising drug and gene delivery systems. *J. Control. Release.* 161, 38-49.

Feng, A.L., Boraey, M.A., Gwin, M.A., Finlay, P.R., Kuehl, P.J., Vehring, R., 2011. Mechanistic models facilitate efficient development of leucine containing microparticles for pulmonary drug delivery. *Int. J. Pharm.* 409, 156-163.

Fu, J., Wiraja, C., Muhammad, H.B., Xu, C., Wang, D.A., 2017. Improvement of endothelial progenitor outgrowth cell (EPOC)-mediated vascularization in gelatin-based hydrogels through pore size manipulation. *Acta. Biomaterialia.* 58, 225-237.

Gao, Y., Zuo, J., Bou-Chacra, N., Pinto Tde, J., Clas, S.D., Walker, R.B., Löbenberg, R., 2013. In vitro release kinetics of antituberculosis drugs from nanoparticles assessed using a modified dissolution apparatus. *Biomed. Res. Int.* 2013:136590.

Genestier, L., Paillot, R., Quemeneur, L., Izeradjene, K., Revillard, J.P., 2000. Mechanisms of action of methotrexate. *Immunopharmacology.* 47, 247-257.

Gill, K.K., Nazzal, S., Kaddoumi, A., 2011. Paclitaxel loaded PEG(5000)-DSPE micelles as pulmonary delivery platform: formulation characterization, tissue distribution, plasma pharmacokinetics, and toxicological evaluation. *Eur. J. Pharm. Biopharm.* 79, 276-284.

Hathout, R.M., Omran, M.K., 2016. Gelatin-based particulate systems in ocular drug delivery. *Pharm. Dev. Technol.* 21, 379-386.

Inoue, K., Yuasa, H., 2014. Molecular basis for pharmacokinetics and pharmacodynamics of methotrexate in rheumatoid arthritis therapy. *Drug Metab. Pharmacokinet.* 29, 12-19.

Jouyban, A., Shaghghi, M., Manzoori, L., Soleymani, J., Jalilvaez-Gharamaleki, J., 2011. Determination of methotrexate in biological fluids and a parenteral injection using terbium-sensitized method. *Iran J. Pharm. Res.* 10, 695-704.

Jyoti, K., Kaur, K., Pandey, R.S., Jain, U.K., Chandra, R., Madan, J., 2015. Inhalable nanostructured lipid particles of 9-bromo-noscapine, a tubulin-binding cytotoxic agent: in vitro and in vivo studies. *J. Colloid Interface Sci.* 445, 219-230.

Kulkarni, S.A., Feng, S.S., 2013. Effects of particle size and surface modification on cellular uptake and biodistribution of polymeric nanoparticles for drug delivery. *Pharm. Res.* 30, 2512-2522.

Kunda, N.K., Alfagih, I.M., Dennison, S.R., Tawfeek, H.M., Somavarapu, S., Hutcheon, G.A., Saleem, I.Y., 2015a. Bovine serum albumin adsorbed PGA-co-PDL nanocarriers for vaccine delivery via dry powder inhalation. *Pharm. Res.* 32, 1341-1353.

Kunda, N.K., Alfagih, I.M., Miyaji, E.N., Figueiredo, D.B., Goncalves, V.M., Ferreira, D.M., Dennison, S.R., Somavarapu, S., Hutcheon, G.A., Saleem, I.Y., 2015b. Pulmonary dry powder vaccine of pneumococcal antigen loaded nanoparticles. *Int. J. Pharm.* 495, 903-912.

Kunda, N.K., Alfagih, I.M., Dennison, S.R., Somavarapu, S., Merchant, Z., Hutcheon, G.A., Saleem, I.Y., 2015c. Dry powder pulmonary delivery of cationic PGA-co-PDL nanoparticles with surface adsorbed model protein. *Int. J. Pharm.* 492, 213-222.

- Leo, E., Cameroni, R., Forni, F., 1999. Dynamic dialysis for the drug release evaluation from doxorubicin-gelatin nanoparticle conjugates. *Int. J. Pharm.* 180, 23-30.
- Luo, F., Li, Y., Jia, M., Cui, F., Wu, H., Yu, F., Lin, J., Yang, X., Hou, Z., Zhang, Q., 2014. Validation of a Janus role of methotrexate-based PEGylated chitosan nanoparticles in vitro. *Nanoscale. Res. Lett.* 9, 363.
- Jahanshahi, M., Sanati, M.H., Babaei, Z., 2008. Optimization of parameters for the fabrication of gelatin nanoparticles by the Taguchi robust design method. *J. Appl. Stat.* 35, 1345-1353.
- Mangal, S., Gao, W., Li, T., Zhou, Q.T., 2017. Pulmonary delivery of nanoparticle chemotherapy for the treatment of lung cancers: challenges and opportunities. *Acta Pharmacol. Sin.* 38, 782-797.
- Marasini, N., Tran, T.H., Poudel, B.K., Choi, H.G., Yong, C.S., Kim, J.O., 2013. Statistical modeling, optimization and characterization of spray-dried solid self-microemulsifying drug delivery system using design of experiments. *Chem. Pharm. Bull.* 61, 184-193.
- Metwally, A.A., El-Ahmady, S.H., Hathout, R.M., 2016. Selecting optimum protein nano-carriers for natural polyphenols using chemoinformatics tools. *Phytomedicine.* 23, 1764-1770.
- Mohanty, B., Aswal, V.K., Kohlbrecher, J., Bohidar, H.B., 2005. Synthesis of Gelatin Nanoparticles via Simple Coacervation. *J. Surface Sci. Technol.* 21, 149-160.
- Nagayasu, A., Uchiyama, K., Kiwada, H., 1999. The size of liposomes: a factor which affects their targeting efficiency to tumors and therapeutic activity of liposomal antitumor drugs. *Adv. Drug Deliv. Rev.* 40, 75-87.
- Naguib, S.S., Hathout, R.M., Mansour, S., 2017. Optimizing novel penetration enhancing hybridized vesicles for augmenting the in-vivo effect of an anti-glaucoma drug. *Drug Deliv.* 24, 99-108.
- Najafabadi, A.R., Gilani, K., Barghi, M., Rafiee-Tehrani, M., 2004. The effect of vehicle on physical properties and aerosolisation behaviour of disodium cromoglycate microparticles spray dried alone or with L-leucine. *Int. J. Pharm.* 285, 97-108.
- Novello, S., Barlesi, F., Califano, R., Cufer, T., Ekman, S., Levra, M.G., Kerr, K., Popat, S., Reck, M., Senan, S., Simo, G.V., Vansteenkiste, J., Peters, S., 2016. Metastatic non-small-cell lung cancer: ESMO Clinical Practice Guidelines for diagnosis, treatment and follow-up. *Ann. Oncol.* 27, v1-v27.
- Oliveira, A.R., Caland, L.B., Oliveira, E.G., Egito, E.S.T., Pedrosa, M.F.F., Silva Júnior, A.A., 2015. HPLC-DAD and UV-Vis Spectrophotometric methods for methotrexate assay in different biodegradable microparticles. *J. Braz. Chem. Soc.* 26, 649-659.
- Osman, R., Kan, P.L., Awad, G., Mortada, N., El-Shamy, A.E., Alpar, O., 2013. Spray dried inhalable ciprofloxacin powder with improved aerosolisation and antimicrobial activity. *Int. J. Pharm.* 449, 44-58.

Padmanabhan, S., Tripathi, D.N., Vikram, A., Ramarao, P., Jena, G.B., 2009. Methotrexate-induced cytotoxicity and genotoxicity in germ cells of mice: intervention of folic and folinic acid. *Mutat. Res.* 673, 43-52.

Park, E.K., Jung, H.S., Yang, H.I., Yoo, M.C., Kim, C., Kim, K.S., 2007. Optimized THP-1 differentiation is required for the detection of responses to weak stimuli. *Inflamm. Res.* 56, 45-50.

Safwat, S., Hathout, R.M., Ishak, R.A., Mortada, N.D., 2017. Augmented simvastatin cytotoxicity using optimized lipid nanocapsules: a potential for breast cancer treatment. *J. Liposome Res.* 27, 1-10.

Seo, D.H., Jeong, Y.I., Kim, D.G., Jang, M.J., Jang, M.K., Nah, J.W., 2009. Methotrexate-incorporated polymeric nanoparticles of methoxy poly(ethylene glycol)-grafted chitosan. *Colloids Surf. B Biointerfaces.* 69, 157-163.

Sham, J.O., Zhang, Y., Finlay, W.H., Roa, W.H., Lobenberg, R., 2004. Formulation and characterization of spray-dried powders containing nanoparticles for aerosol delivery to the lung. *Int. J. Pharm.* 269, 457-467.

Shin, J.M., Kim, S.H., Thambi, T., You, D.G., Jeon, J., Lee, J.O., Chung, B.Y., Jo, D.G., Park, J.H., 2014. A hyaluronic acid-methotrexate conjugate for targeted therapy of rheumatoid arthritis. *Chem. Commun. (Camb.)*. 50, 7632-7635.

Shutava, T.G., Balkundi, S.S., Vangala, P., Steffan, J.J., Bigelow, R.L., Cardelli, J.A., O'Neal, D.P., Lvov, Y.M., 2009. Layer-by-Layer-Coated Gelatin Nanoparticles as a Vehicle for Delivery of Natural Polyphenols. *ACS Nano.* 3, 1877-1885.

Sou, T., Kaminskis, L.M., Nguyen, T.H., Carlberg, R., McIntosh, M.P., Morton, D.A., 2013. The effect of amino acid excipients on morphology and solid-state properties of multi-component spray-dried formulations for pulmonary delivery of biomacromolecules. *Eur. J. Pharm. Biopharm.* 83, 234-243.

Takashiba, S., Van Dyke, T.E., Amar, S., Murayama, Y., Soskolne, A.W., Shapira, L., 1999. Differentiation of monocytes to macrophages primes cells for lipopolysaccharide stimulation via accumulation of cytoplasmic nuclear factor kappaB. *Infect. Immun.* 67, 5573-5578.

Taratula, O., Garbuzenko, O.B., Chen, A.M., Minko, T., 2011. Innovative strategy for treatment of lung cancer: targeted nanotechnology-based inhalation co-delivery of anticancer drugs and siRNA. *J. Drug Target.* 19, 900-914.

Tawfeek, H., Khidr, S., Samy, E., Ahmed, S., Murphy, M., Mohammed, A., Shabir, A., Hutcheon, G., Saleem, I., 2011. Poly(glycerol adipate-co-omega-pentadecalactone) spray-dried microparticles as sustained release carriers for pulmonary delivery. *Pharm. Res.* 28, 2086-2097.

Tawfeek, H.M., Evans, A.R., Iftikhar, A., Mohammed, A.R., Shabir, A., Somavarapu, S., Hutcheon, G.A., Saleem, I.Y., 2013. Dry powder inhalation of macromolecules using novel PEG-co-polyester microparticle carriers. *Int. J. Pharm.* 441, 611-619.

The, T.H., Feltkamp, T.E.W., 1970. Conjugation of fluorescein isothiocyanate to antibodies: I. Experiments on the conditions of conjugation. *Immunology* 18, 865-873.

Wong, C., Stylianopoulos, T., Cui, J., Martin, J., Chauhan, V.P., Jiang, W., Popovic, Z., Jain, R.K., Bawendi, M.G., Fukumura, D., 2011. Multistage nanoparticle delivery system for deep penetration into tumor tissue. *Proc. Natl. Acad. Sci. USA.* 108, 2426-2431.

Yang, F., Liu, X., Wang, W., Liu, C., Quan, L., Liao, Y., 2015. The effects of surface morphology on the aerosol performance of spray-dried particles within HFA 134a based metered dose formulations. *Asian J. Pharm. Sci.* 10, 513-519.

Yang, W., Peters, J.I., Williams, R.O., III, 2008. Inhaled nanoparticles--a current review. *Int. J. Pharm.* 356, 239-247.

Zhang, T., Youan, B.B., 2010. Analysis of process parameters affecting spray-dried oily core nanocapsules using factorial design. *AAPS PharmSciTech.* 11, 1422-1431.

Zwioerek, K., Bourquin, C., Battiany, J., Winter, G., Endres, S., Hartmann, G., Coester, C., 2008. Delivery by cationic gelatin nanoparticles strongly increases the immunostimulatory effects of CpG oligonucleotides. *Pharm. Res.* 25, 551-562.

Zwioerek, K., Kloeckner, J., Wagner, E., Coester, C., 2005. Gelatin nanoparticles as a new and simple gene delivery system. *J. Pharm. Pharm. Sci.* 7, 22-28.

**Table 1.** Process parameters used in the Box Behnken design for optimizing GNPs fabrication conditions.

| <b>Parameter</b>             | <b>Unit</b>   | <b>1</b> | <b>2</b> | <b>3</b> |
|------------------------------|---------------|----------|----------|----------|
| Stirring speed               | rpm           | 800      | 1200     | 1600     |
| Crosslinking time            | Hour          | 8        | 12       | 16       |
| Crosslinking solution volume | $\mu\text{L}$ | 99       | 165      | 231      |

**Table 2.** Structure of Box-Behnken design with the corresponding experimentally determined particle size results of the prepared GNPs.

| Run | Stirring speed (rpm) | Crosslinking time (h) | Crosslinking solution volume ( $\mu\text{L}$ ) | Particle size (nm) |
|-----|----------------------|-----------------------|--|--------------------|
| 1   | 1                    | 2                     | 1  | 282.33 $\pm$ 3.95  |
| 2   | 1                    | 2                     | 3  | 247.20 $\pm$ 4.59  |
| 3   | 3                    | 2                     | 3  | 180.31 $\pm$ 10.10 |
| 4   | 1                    | 1                     | 2  | 373.36 $\pm$ 7.04  |
| 5   | 2                    | 1                     | 1  | 469.56 $\pm$ 7.37  |
| 6   | 3                    | 1                     | 2  | 299.91 $\pm$ 13.45 |
| 7   | 2                    | 2                     | 2  | 262.83 $\pm$ 4.55  |
| 8   | 1                    | 3                     | 2  | 316.73 $\pm$ 3.13  |
| 9   | 3                    | 3                     | 2  | 224.20 $\pm$ 5.54  |
| 10  | 2                    | 1                     | 3  | 265.83 $\pm$ 6.10  |
| 11  | 2                    | 3                     | 1  | 266.46 $\pm$ 6.31  |
| 12  | 3                    | 2                     | 1  | 271.73 $\pm$ 8.33  |
| 13  | 2                    | 3                     | 3  | 306.06 $\pm$ 6.91  |
| 14  | 2                    | 2                     | 2  | 273.70 $\pm$ 7.75  |
| 15  | 2                    | 2                     | 2  | 269.43 $\pm$ 3.28  |

Results are expressed as (Mean  $\pm$  SD, n=3)

**Table 3.** Characteristics of fabricated gelatin NPs.

| <b>Formulas</b>               | <b>Size (nm)</b>   | <b>PDI</b>       | <b>Zeta potential (mV)</b> | <b>Drug loading (<math>\mu\text{g}/\text{mg}</math>)</b> |
|-------------------------------|--------------------|------------------|----------------------------|--|
| Plain NPs                     | 180.31 $\pm$ 10.10 | 0.05 $\pm$ 0.030 | 18.50 $\pm$ 1.81           |  |
| Cationized plain NPs (pH 8)   | 217.78 $\pm$ 23.92 | 0.08 $\pm$ 0.047 | 18.08 $\pm$ 1.02           |  |
| FITC-labelled NPs             | 188.00 $\pm$ 6.20  | 0.07 $\pm$ 0.003 | -20.00 $\pm$ 1.20          |  |
| Encapsulated MTX NPs          | 303.38 $\pm$ 3.30  | 0.14 $\pm$ 0.008 | 17.21 $\pm$ 0.17           | 4.10 $\pm$ 0.39  |
| Post Loaded MTX NPs           | 255.70 $\pm$ 5.92  | 0.14 $\pm$ 0.010 | 14.03 $\pm$ 0.05           | 96.00 $\pm$ 3.41   |
| Chemically Conjugated MTX NPs | 148.45 $\pm$ 2.49  | 0.05 $\pm$ 0.020 | -22.56 $\pm$ 0.43          | 84.60 $\pm$ 0.23   |

Results are expressed as (Mean  $\pm$  SD, n=3).

**Table 4.** Median FLA-1 values for control and treated cells with FITC – labelled gelatin NPs.

| Cells       | Control cells | Treated cells    |
|-------------|---------------|------------------|
| A549        | 7180 ± 20     | 1,709,633 ± 1080 |
| Macrophages | 2408 ± 60     | 40385 ± 154      |

Control cells are untreated cells with FITC-NPs, results are expressed as (Mean ± SD, n=3).

## Figure Titles

**Fig. 1.** Chemical structure of methotrexate.

**Fig. 2.** Contour plots (right panels) and 3D surfaces (left panels) generated by Box- Behnken design representing the effect of **a**-glutaraldehyde volume (GA), **b**-crosslinking time at different stirring speed at: 800 rpm (Upper panels), 1200 rpm (Middle panels) and 1600 rpm (Lower panels) on the particle size of the fabricated gelatin nanoparticles. Particle size decreases from red to blue color.

**Fig. 3. (A)** Effect of pH on the zeta potential of gelatin NPs and cationized gelatin NPs. **(B)** Effect of MTX concentration and **(C)** stirring time on the loading of MTX on cationized gelatin nanoparticles (Mean  $\pm$  SD, n=3).

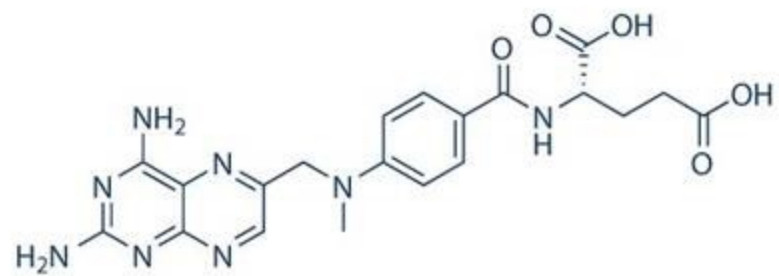
**Fig. 4.** H-NMR spectra for MTX and chemically conjugated MTX. All were dissolved in D<sub>2</sub>O.

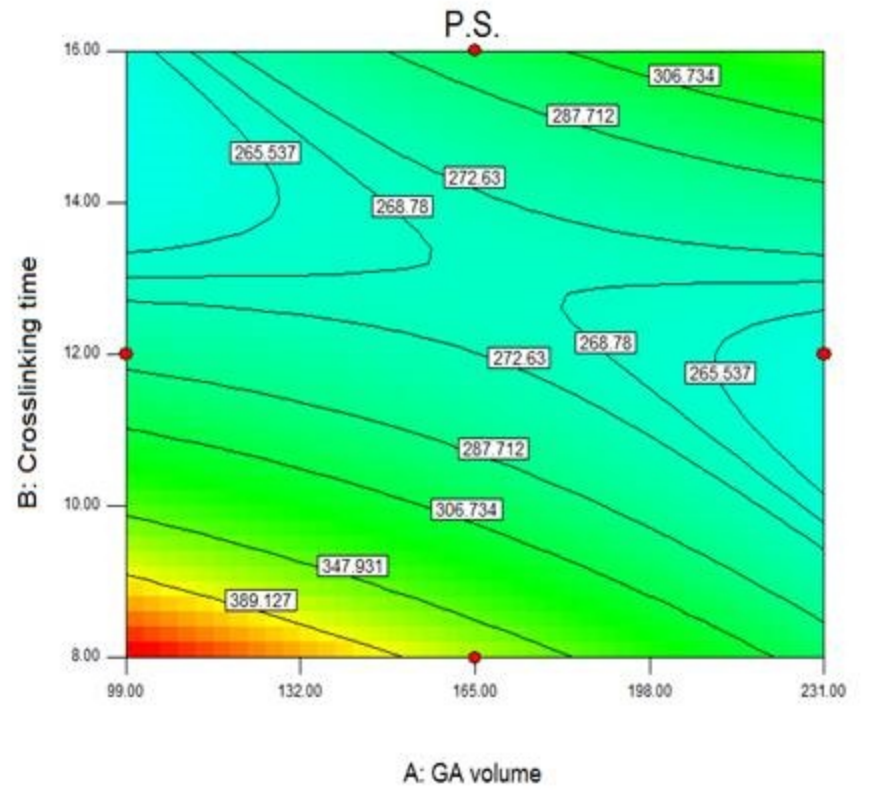
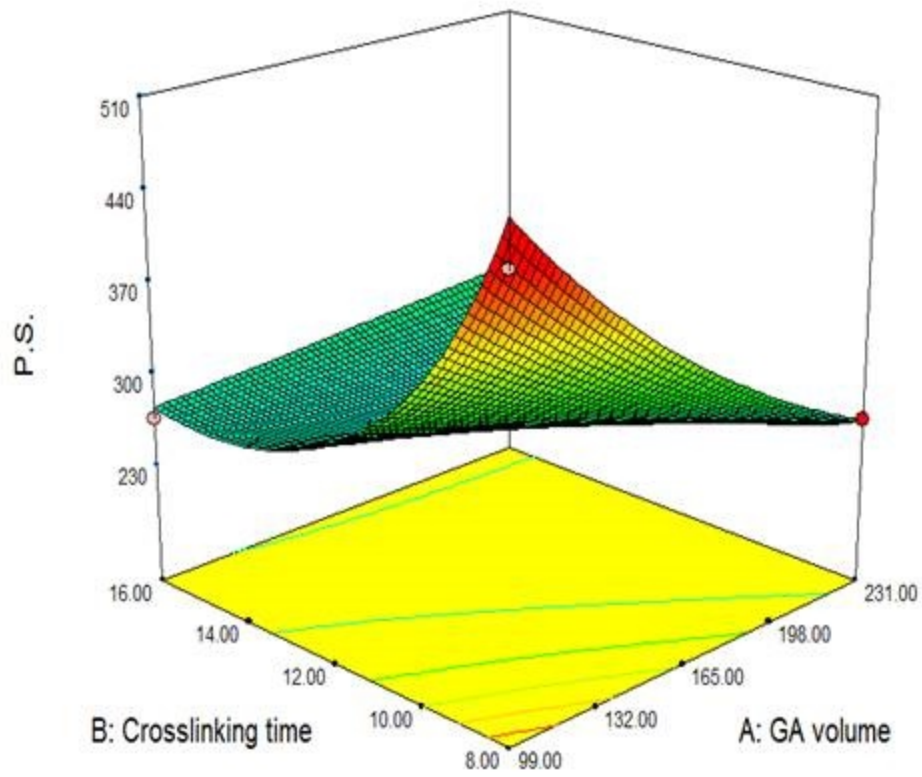
**Fig. 5.** *In-vitro* release profiles for MTX post loaded NPs and MTX chemically conjugated NPs in absence and presence of trypsin in phosphate buffer pH 7.4 (Mean  $\pm$  SD, n=3).

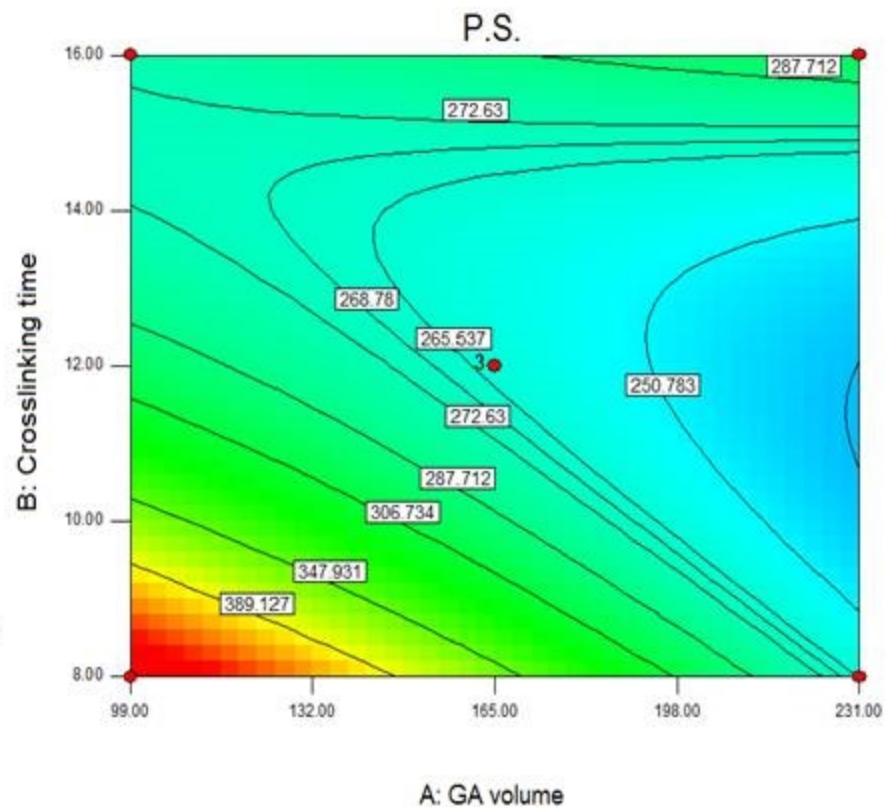
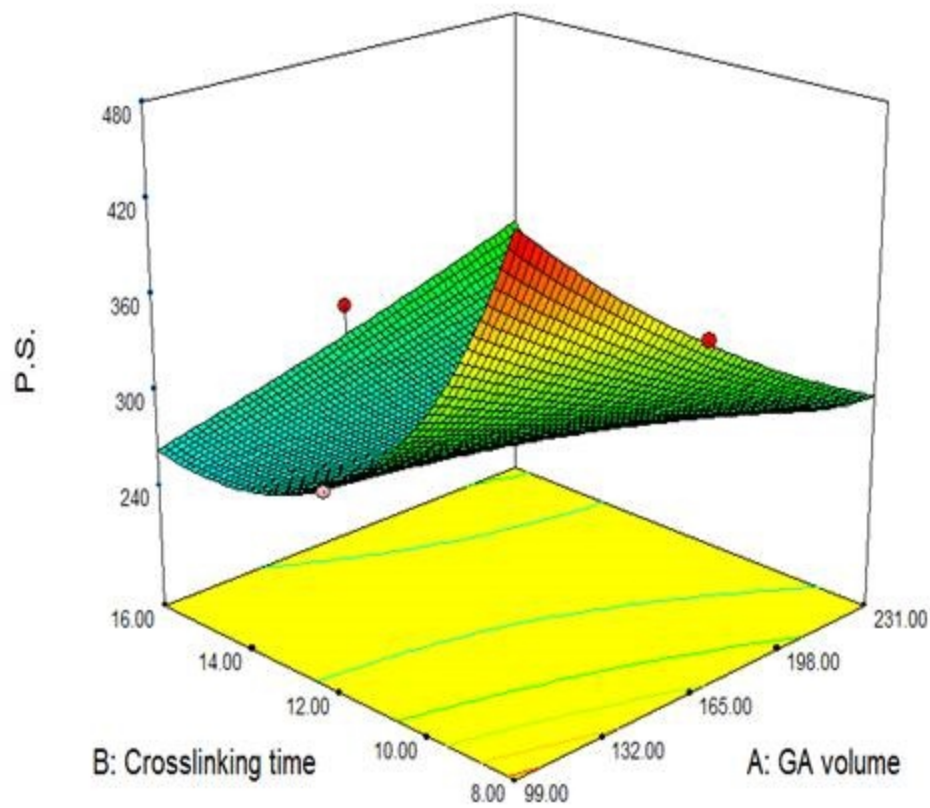
**Fig. 6.** The fluorescence changes of the cells before and after treatment with FITC-labelled GNPs indicating the enhanced uptake into the A549 cells compared to the macrophage cells. **(A)** macrophage cells, **(B)** macrophage cells treated with FITC-labelled GNPs, **(C)** A549 cells, **(D)** A549 cells treated with FITC-labelled GNPs.

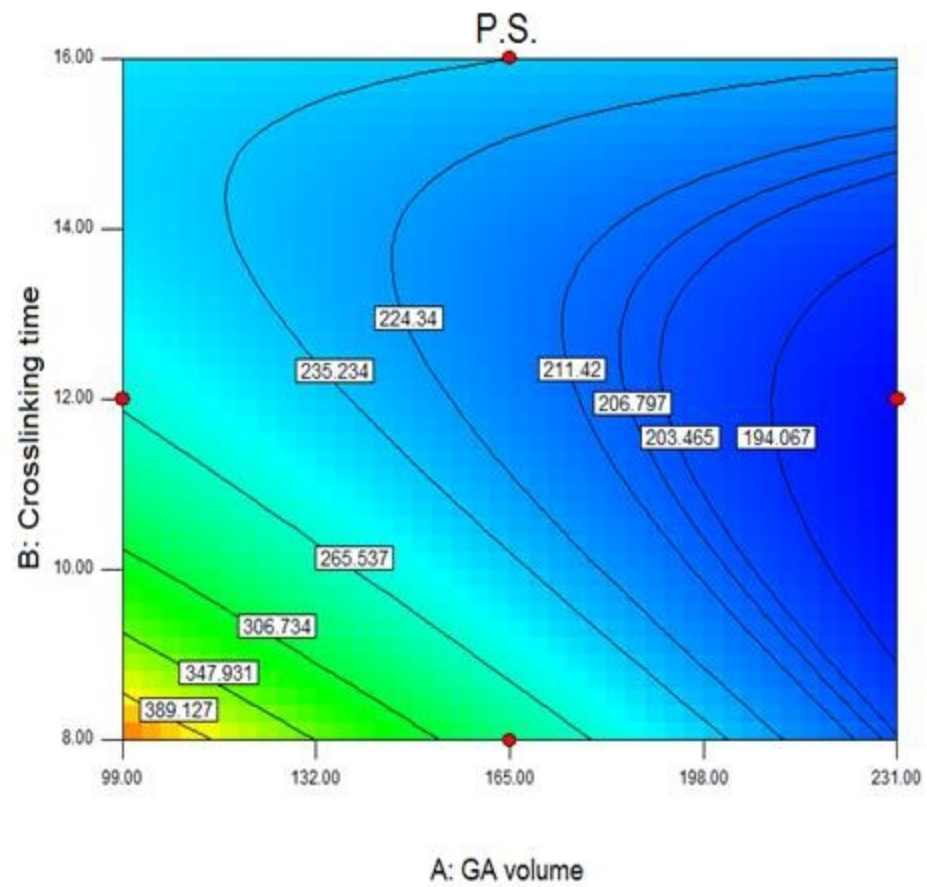
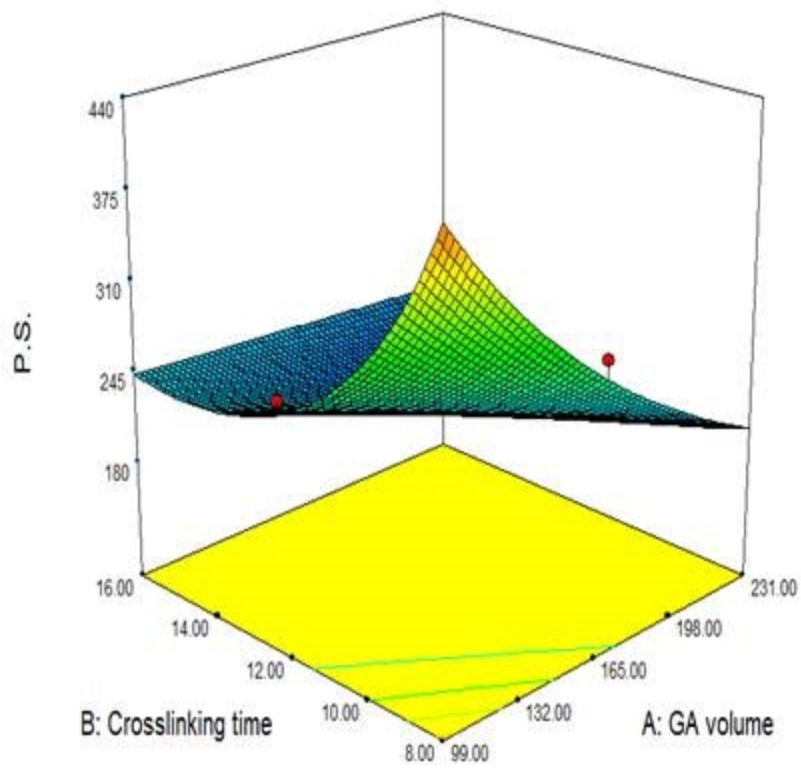
**Fig. 7.** *In-vitro* cytotoxicity profiles for MTX, post loaded and chemically conjugated nanoparticles. (Mean  $\pm$  SD, n=3).

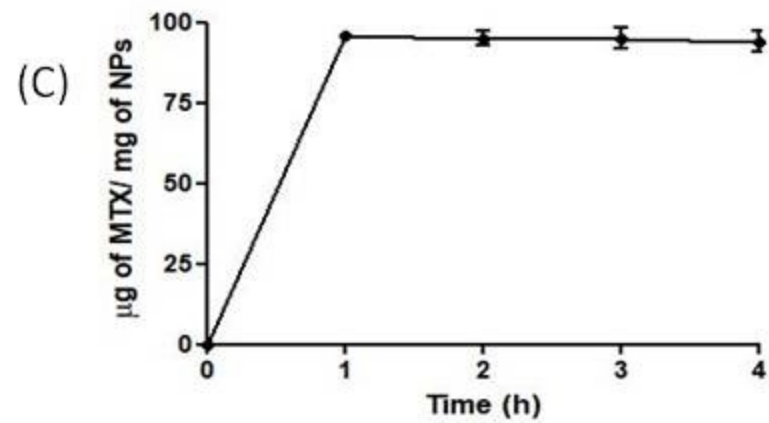
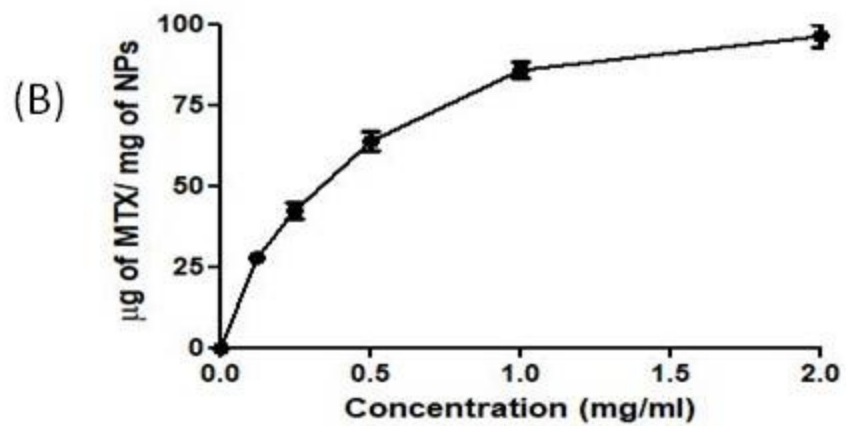
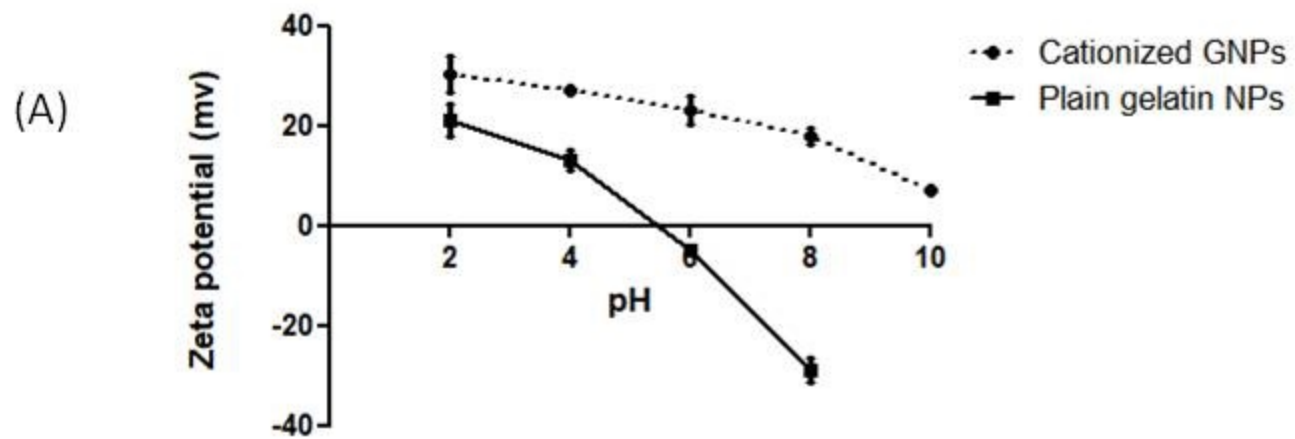
**Fig. 8.** SEM micrographs of MTX chemically conjugated GNPs/NCMPs **(A)** and **(B)** (scale bar 20 & 5  $\mu$ m respectively), TEM images of MTX chemically conjugated GNPs **(C)** before and **(D)** after re-dispersion from spray dried GNPs/NCMPs (scale bar 200 nm).



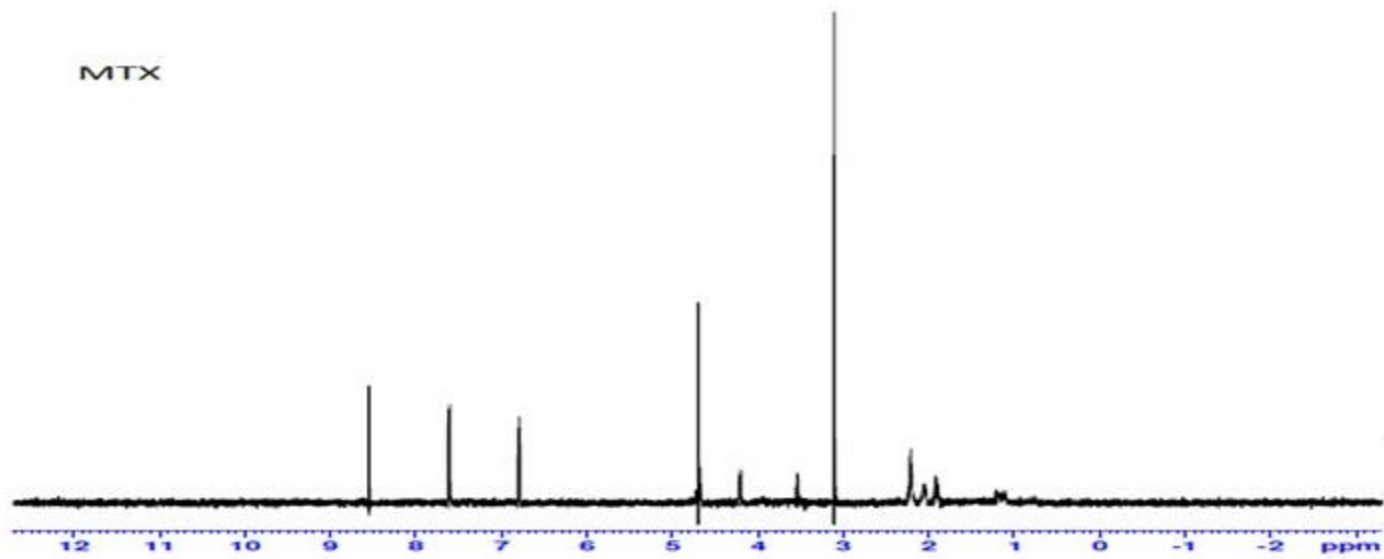




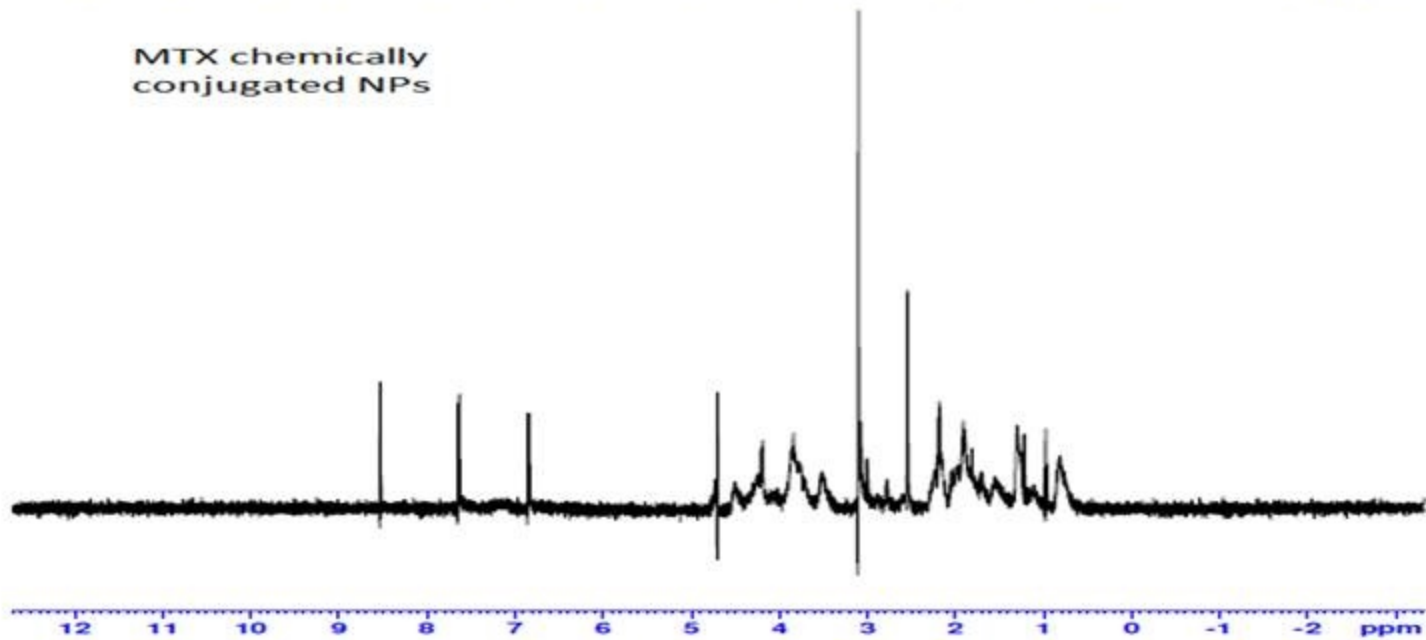


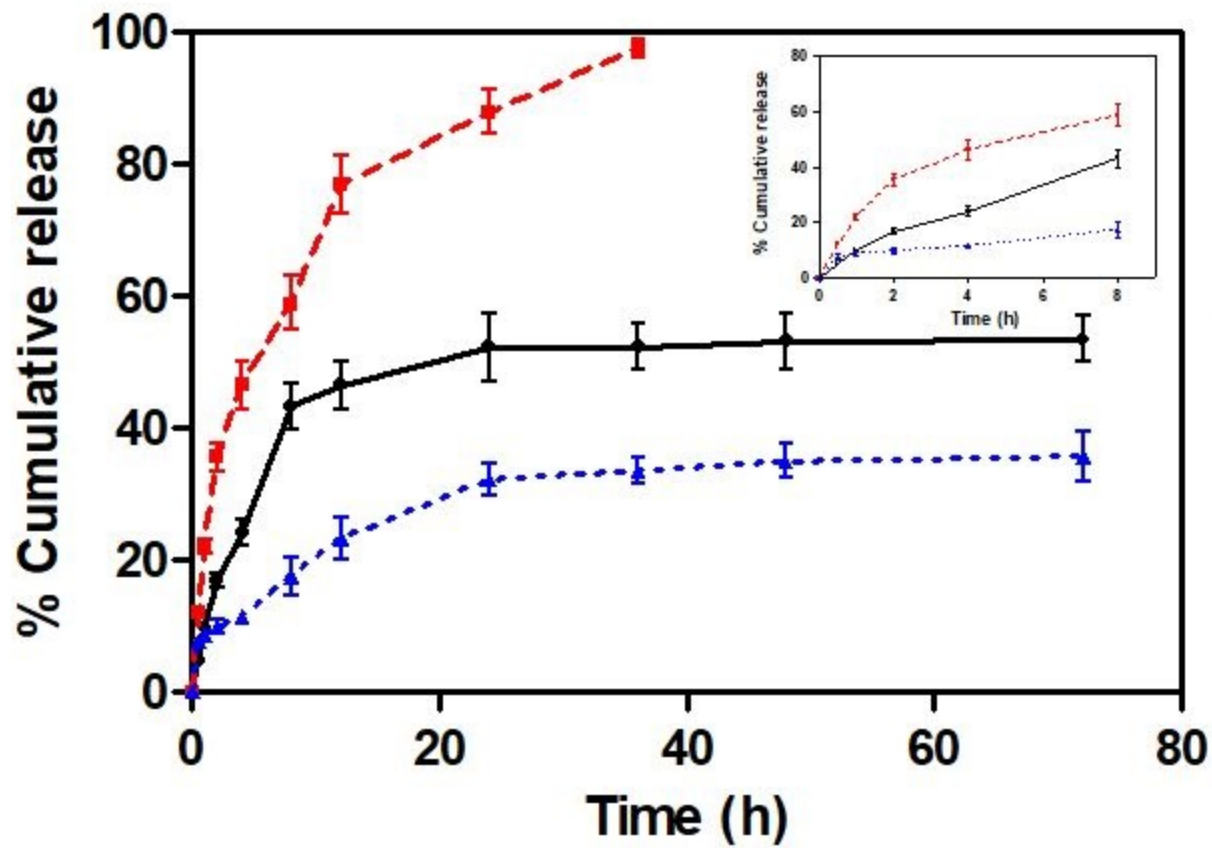


MTX

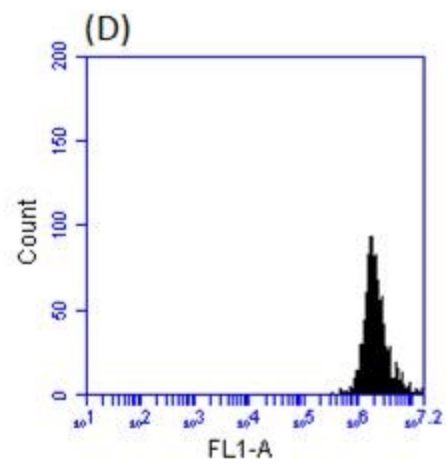
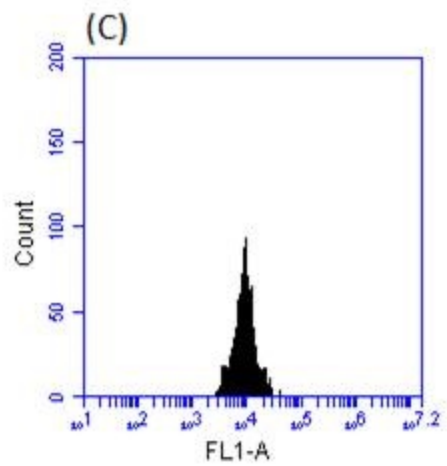
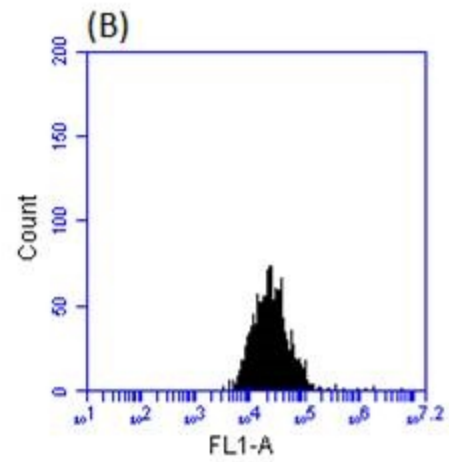
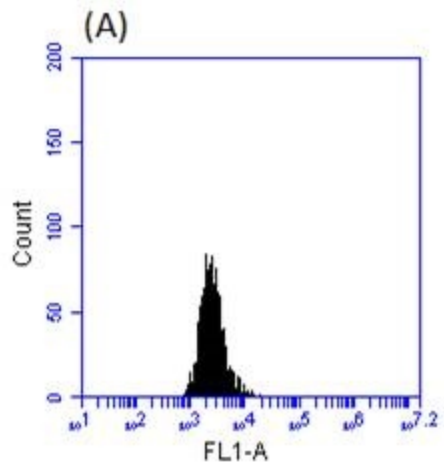


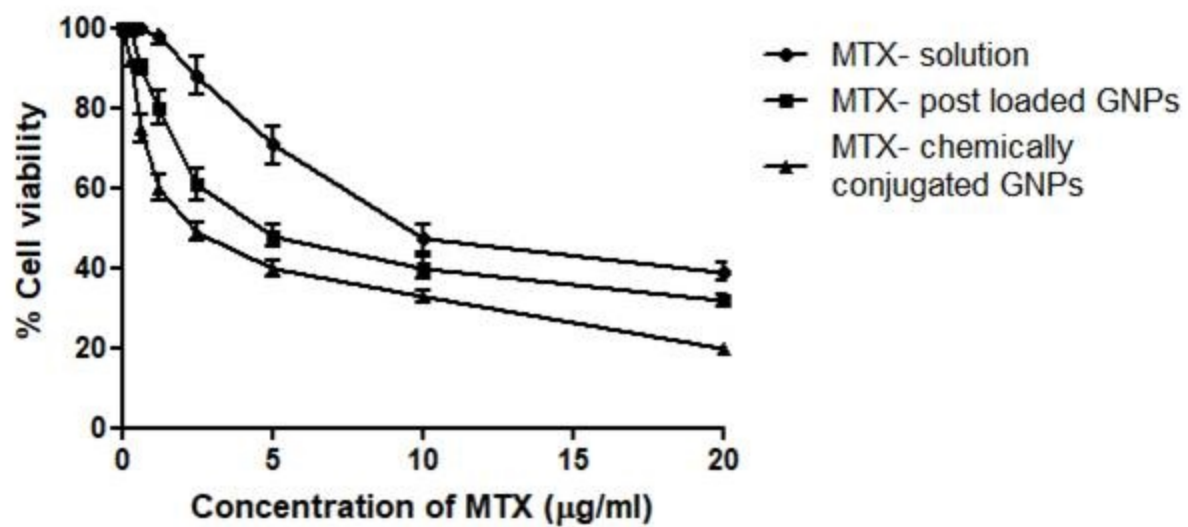
MTX chemically  
conjugated NPs



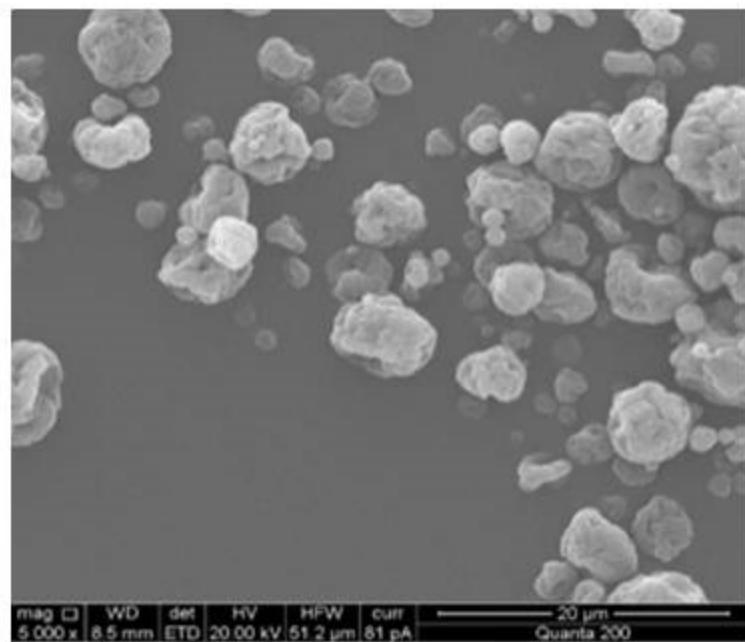


- MTX post loaded GNPs with trypsin
- MTX post loaded GNPs
- ▲— MTX chemically conjugated GNPs with trypsin

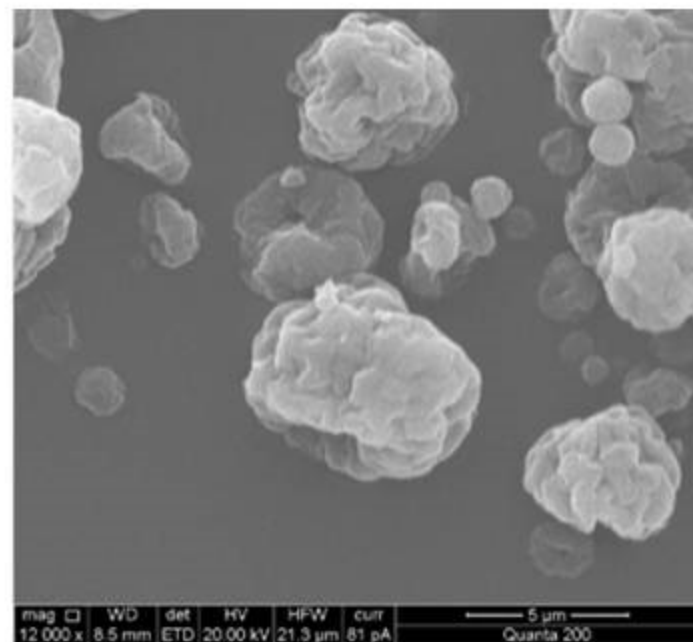




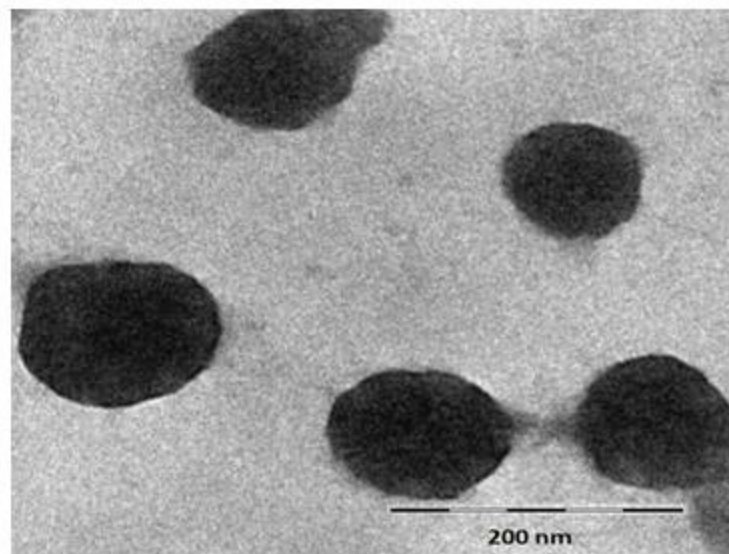
(A)



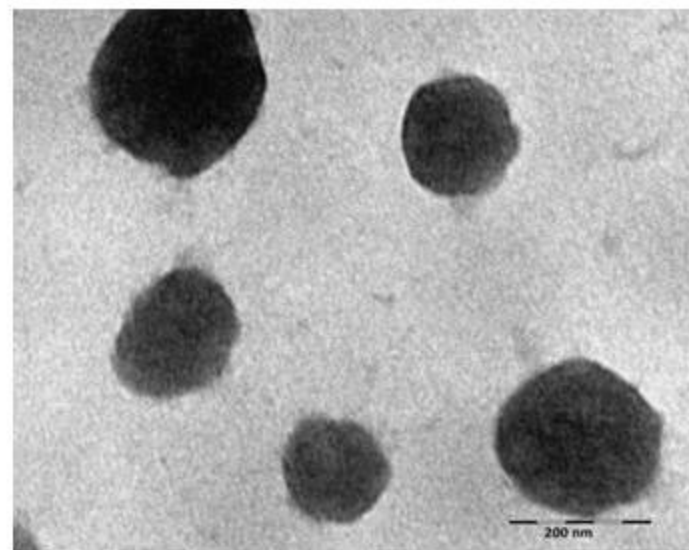
(B)



(C)



(D)



Supplementary material

**Supplementary Table 1.** Regression analysis parameters for GNPs particle size model

| <b>Parameter</b>         | <b>Value</b> |
|--------------------------|--------------|
| ANOVA p-value            | 0.0001       |
| Lack of fit p-value      | 0.0790       |
| R <sup>2</sup>           | 0.9639       |
| Adjusted R <sup>2</sup>  | 0.9368       |
| Predicted R <sup>2</sup> | 0.8678       |
| Adequate precision       | 24.848       |

**Supplementary Table 2.** Experimentally determined yield and residual moisture content for spray dried gelatin NCMPs

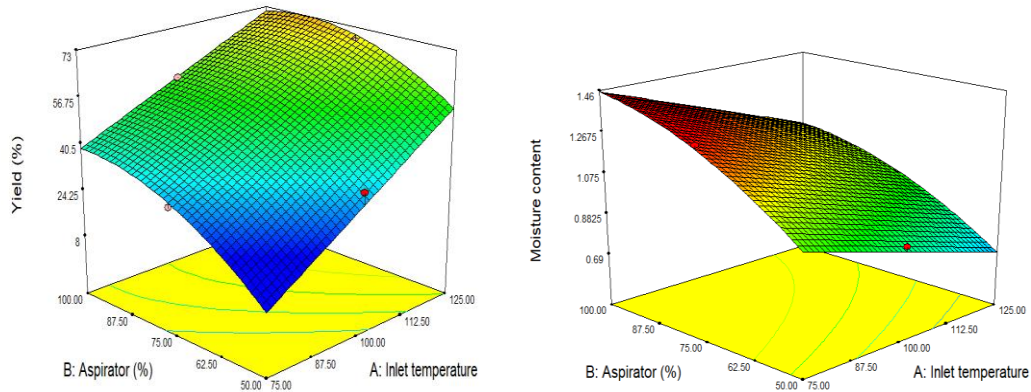
| <b>Run</b> | <b>Inlet temperature (°C)</b> | <b>Aspirator rate (%)</b> | <b>Feed concentration (mg/mL)</b> | <b>Yield (%)</b> | <b>Residual moisture (%)</b> |
|------------|-------------------------------|---------------------------|-----------------------------------|------------------|------------------------------|
| 1          | 75                            | 75                        | 4                                 | 30.0 ± 5.30      | 1.32 ± 0.50                  |
| 2          | 100                           | 50                        | 12                                | 42.0 ± 4.75      | 0.69 ± 0.12                  |
| 3          | 75                            | 100                       | 8                                 | 63.0 ± 7.70      | 1.25 ± 0.35                  |
| 4          | 100                           | 75                        | 8                                 | 64.0 ± 2.50      | 1.01 ± 0.07                  |
| 5          | 100                           | 100                       | 4                                 | 55.0 ± 9.40      | 1.26 ± 0.08                  |
| 6          | 100                           | 100                       | 12                                | 79.0 ± 9.70      | 1.13 ± 0.43                  |
| 7          | 75                            | 75                        | 12                                | 61.0 ± 6.10      | 1.07 ± 0.51                  |
| 8          | 100                           | 75                        | 8                                 | 66.0 ± 3.50      | 0.98 ± 0.19                  |
| 9          | 125                           | 100                       | 8                                 | 84.5 ± 6.80      | 0.98 ± 0.28                  |
| 10         | 100                           | 75                        | 8                                 | 65.0 ± 2.40      | 1.03 ± 0.10                  |
| 11         | 100                           | 50                        | 4                                 | 35.0 ± 5.50      | 0.87 ± 0.21                  |
| 12         | 75                            | 50                        | 8                                 | 19.0 ± 5.90      | 0.78 ± 0.14                  |
| 13         | 125                           | 75                        | 4                                 | 68.0 ± 1.40      | 0.95 ± 0.05                  |
| 14         | 125                           | 50                        | 8                                 | 53.0 ± 3.20      | 0.56 ± 0.05                  |
| 15         | 125                           | 75                        | 12                                | 76.0 ± 4.80      | 0.78 ± 0.07                  |

**Supplementary Table 3.** Regression analysis and equation for yield and residual moisture responses for spray drying designated model

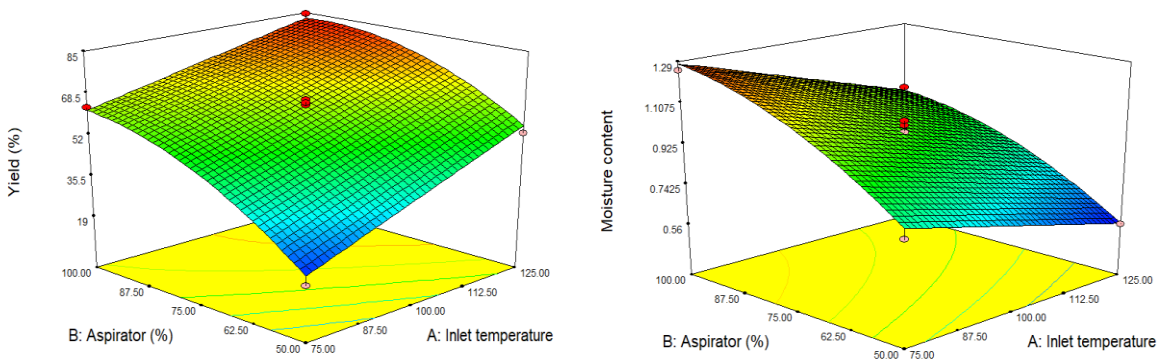
| <b>Parameter</b>         | <b>Yield</b>           | <b>Residual moisture</b> |
|--------------------------|------------------------|--------------------------|
| ANOVA p-value            | 0.0002                 | 0.0002                   |
| Lack of fit p-value      | 0.0555                 | 0.2644                   |
| R <sup>2</sup>           | 0.9890                 | 0.9895                   |
| Adjusted R <sup>2</sup>  | 0.9692                 | 0.9707                   |
| Predicted R <sup>2</sup> | 0.8296                 | 0.8592                   |
| Adequate precision       | 22.709                 | 24.459                   |
| Model equation           | Yield=                 | Moisture content=        |
|                          | =                      | +0.98                    |
|                          | +63.73                 | -0.14 * A                |
|                          | +13.56 * A             | +0.22 * B                |
|                          | +16.56 * B             | -0.091 * C               |
|                          | +8.75 * C              | -0.013 * A * B           |
|                          | -3.13 * A * B          | +0.020 * A * C           |
|                          | -5.75 * A * C          | -0.076 * B <sup>2</sup>  |
|                          | +4.25 * B * C          | +0.062 * C <sup>2</sup>  |
|                          | -7.90 * B <sup>2</sup> |                          |
|                          | -4.0 * C <sup>2</sup>  |                          |

Where A is inlet temperature, B is aspirator % and C is feed concentration.

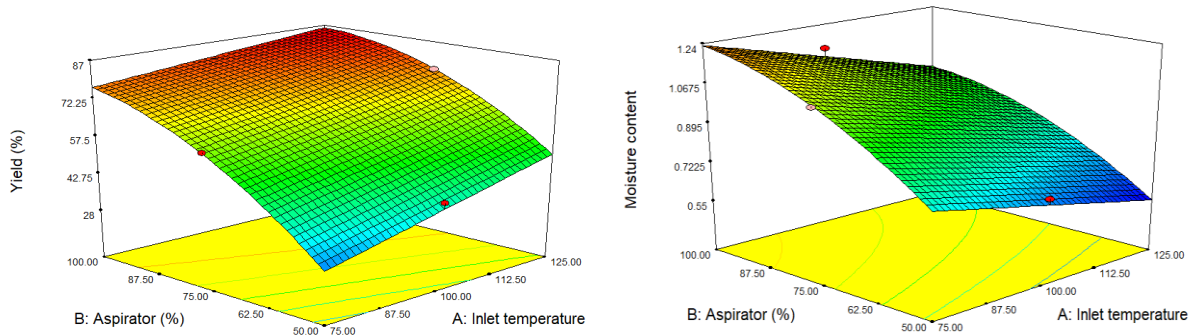
(A)



(B)



(C)



**Supplementary Fig. 1.** 3D surfaces generated by Box Behnken design representing the effect of inlet temperature and aspirator (%) at different feed concentration at (A) 4mg/mL (Upper panels), (B) 8 mg/mL (Middle panels) and (C) 12mg/mL (Lower panels) on the yield (%) (Right panels) and moisture content (Left panels) of spray dried NCMPs. Yield (%) and moisture content decrease from red to blue color.